Biomedicine & Pharmacotherapy 164 (2023) 114879

Contents lists available at ScienceDirect

Biomedicine & Pharmacotherapy

journal homepage: www.elsevier.com/locate/biopha

Multi-target withaferin-A analogues as promising anti-kinetoplastid agents through the programmed cell death

Desirée San Nicolás-Hernández [a,b], Eduardo Hernández-Álvarez [c], Carlos J. Bethencourt-Estrella [a,b], Atteneri López-Arencibia [a,b,*], Ines Sifaoui [a,b], Isabel L. Bazzocchi [c], Jacob Lorenzo-Morales [a,b], Ignacio A. Jiménez [c,**], José E. Piñero [a,b]

[a] Instituto Universitario de Enfermedades Tropicales y Salud Pública de Canarias, Universidad de La Laguna, Avenida Astrofísico Francisco Sánchez, S/N, 38203 La Laguna, Tenerife, Canary Islands, Spain
[b] Departamento de Obstetricia y Ginecología, Pediatría, Medicina Preventiva y Salud Pública, Toxicología, Medicina Legal y Forense y Parasitología, Universidad de La Laguna, 38200 La Laguna, Tenerife, Spain
[c] Instituto Universitario de Bio-Orgánica Antonio González, Departamento de Química Orgánica, Universidad de La Laguna, Avenida Astrofísico Francisco Sánchez 2, 38206 La Laguna, Tenerife, Canary Islands, Spain

ARTICLE INFO

Keywords:
Withaferin A analogues
Leishmaniasis
Chagas disease
Chemotherapy
Apoptosis-like
Autophagy

ABSTRACT

Leishmaniasis and Chagas disease, two of the most prevalent neglected tropical diseases, are a world health problem. The harsh reality of these infective diseases is the absence of effective and safe therapies. In this framework, natural products play an important role in overcoming the current need to development new anti-parasitic agents. The present study reports the synthesis, antikinetoplastid screening, mechanism study of fourteen withaferin A derivatives (**2**-**15**). Nine of them (**2**-**6**, **8**-**10** and **12**) showed a potent dose-dependent inhibitory effect on the proliferation of *Leishmania amazonensis* and *L. donovani* promastigotes and *Trypanosoma cruzi* epimastigotes with IC_{50} values ranging from 0.19 to 24.01 μM. Outstandingly, the fully acetylated derivative **10** (4,27-diacetylwithaferin A) was the most potent compound showing IC_{50} values of 0.36, 2.82 and 0.19 μM against *L. amazonensis*, *L. donovani* and *T. cruzi*, respectively. Furthermore, analogue **10** exhibited approximately 18 and 36-fold greater antikinetoplastid activity, on *L. amazonensis* and *T. cruzi*, than the reference drugs. The activity was accompanied by significantly lower cytotoxicity on the murine macrophage cell line. Moreover, compounds **2**, **3**, **5**-**7**, **9** and **10** showed more potent activity than the reference drug against the intracellular amastigotes forms of *L. amazonensis* and *T.cruzi*, with a good selectivity index on a mammalian cell line. In addition, withaferin A analogues **3**, **5**-**7**, **9** and **10** induce programmed cell death through a process of apoptosis-like and autophagy. These results strengthen the anti-parasitic potential of withaferin A-related steroids against neglected tropical diseases caused by *Leishmania* spp. and *T. cruzi* parasites.

1. Introduction

Neglected tropical diseases (NTDs), also known as diseases of poverty since they disproportionately affect poor and marginalized populations, are prevalent in tropical and subtropical regions of Africa, America, Asia, and Oceania. NTDs continue to affect more than 1 billion people/year, and the incidence and mortality of this NTDs are rapidly growing worldwide, causing tremendous threat to human life and health. Moreover, in recent decades it is becoming a burden, especially in the United States and Europe, due to global change, in particular climate change [1]. Leishmaniasis and Chagas disease are two of the most important NTDs according to the World Health Organization (WHO) caused by several species of intracellular kinetoplastid parasites and they can result in epidemic outbreaks [1,2].

Abbreviations: WA, withaferin A; DMSO, dimethyl sulfoxide; PI, propidium iodide; PCD, programmed cell death; ROS, reactive oxygen species; MCD, monodansylcadaverine.

* Corresponding author at: Instituto Universitario de Enfermedades Tropicales y Salud Pública de Canarias, Universidad de La Laguna, Avenida Astrofísico Francisco Sánchez, S/N, 38203 La Laguna, Tenerife, Canary Islands, Spain.
** Corresponding author.
E-mail addresses: atlopez@ull.edu.es (A. López-Arencibia), ignadiaz@ull.edu.es (I.A. Jiménez).

https://doi.org/10.1016/j.biopha.2023.114879
Received 31 March 2023; Received in revised form 9 May 2023; Accepted 12 May 2023
Available online 19 May 2023

The leishmaniasis constitutes a group of human and animal diseases caused by several *Leishmania* species, a protozoan parasite from the Trypanosomatidae family. The transmission is prevalent in 98 countries with most cases occurring in South and Central America, the Mediterranean Basin and extending across the Middle East to Central Asia. There are 350 million people at risk and 12 million cases of infection every year [3]. On the other hand, Chagas disease, also known as American Trypanosomiasis, is a zoonotic infection disease caused by the protozoan parasite *Trypanosoma cruzi*. This disease is considered endemic illness in all South and Central America, affecting between 6 and 7 million people worldwide [4].

Treatment of leishmaniasis depends primarily on the characteristics of the parasite and the host. In most cases, different therapeutic strategies are applied depending on the species of *Leishmania* causing the disease and the geographical region where the disease was acquired. Nowadays, the reference drugs used against leishmaniasis are pentavalent antimonials, amphotericin B, pentamidine, paramomycin and miltefosine. Miltefosine is the only orally administered treatment. In the case of Chagas disease, treatment has been based on the use of two drugs since 1960: benznidazole and nifurtimox, the latter being the least safe. At this time, there is no approved vaccine against Chagas disease and leishmaniasis, therefore current treatments for these parasitosis are limited. Moreover, none of the current therapeutic options can be considered ideal due to their high cost and side effects, including teratogenicity and acute toxicity, which often lead to non-adherence [2, 5–8]. These drawbacks of conventional chemical therapy and the absence of a vaccine highlight the urgent need for the development of new agents for antiparasitic chemotherapy of these two diseases. Natural products, as the richest source of active ingredients, are an indispensable tool in the discovery and development of new drugs, especially for the treatment of cancer and infectious diseases [9]. In this sense, withanolides, natural ergostane-type steroid δ-lactone, have attracted much interest due to their structural diversity and broad range of biological activities [10]. Among the withanolides isolated to date, withaferin A (WA) has attracted the most interest due to its broad therapeutic potential to treat multiple ailments and is a promising drug candidate for cancer chemotherapy [11,12].

Apoptosis-like and autophagy are essential and complex biological process in unicellular organisms such as kinetoplastids. Therefore, altering one or both types of programmed cell death could affect the progression of parasite growth, so altering these processes could be a good therapeutic target for the discovery and development of new drugs or anti-parasitic agents [13,14].

During our drug discovery program from Canary Islands biodiversity, we focused our search in *Withania aristata* (Ait.) Pauq. (Solanaceae). This endemic species, popularly known as "orobal", has long been used in traditional medicine. In previous research on *W. aristata*, work was done on the isolation of bioactive molecules, chemical modifications made to them and the biological activities reported for all the withanolides mentioned [15–17]. Recently, we reported three known withanolides that were isolated by bioassay-guided fractionation against *Leishmania* spp. and *Trypanosoma cruzi*, which were obtained from the acetone extract of *W. aristata* leaves, and whose results revealed WA to be a promising compound for further studies [18].

Therefore, motivated by previous work highlighting the role of WA as an anti-parasitic agent [19,20], efforts have been made in this work to expand the biological space of WA and its derivatives to increase their clinical potential as anti-kinetoplastid agents. The present study reports the evaluation of fourteen WA analogues against *L. amazonensis*, *L. donovani* and *T. cruzi* strains, always using the lead compound and reference drugs as comparators against both parasitic diseases. In addition, the ability of six of the analogues to induce programmed cell death in the treated parasites was investigated.

2. Results and discussion

2.1. Chemistry

This study focused on structural optimization of the WA (**1**) antiparasitic profile and gaining insight into the structure-activity relationships (SARs) of withanolide-type steroids as potential antikinetoplastid agents. WA, the main withasteroid in *Withania aristata* leaf extract [15], is primarily responsible for anti-leishmanial and anti-trypanosomal activities [18], so its characteristic structure makes it ideal as a starting material for optimising its anti-parasitic profile.

Chemical structure analysis of WA steroid-backbone suggests four suitable positions for its optimisation through structure-activity relationship (SAR) studies: (i) the hydroxyl groups at C-4 and C-27 positions, (ii) the α,β-unsaturated ketone group, (iii) the α,β-unsaturated δ-lactone, and (iv) the 5β,6β epoxide moiety. Thus, based on the WA skeleton, the series of analogues (**2-15**) were synthesised by standard reactions, which were divided into three groups (Scheme **1**). Therefore, the first step in this work was to study the role of hydroxyl groups at C-4 and C-27, compounds **2-13** were prepared by acylation of WA with alkyl or aryl acid chlorides and alkyl anhydrides of different sizes, lipophilicity and stereoelectronic properties. Secondly, modification on the enone-system and δ-lactone was carried out by epoxidation of double bound of WA at C-2/C-3 and C-24/C-25 (analogues **14**). Finally, the halohydrin **15** was obtained by epoxide ring opening, Supporting Information (S1).

Among the analogues, four out of twelve are reported for the first time: derivatives **2**, **3**, **9** and **11**. The structures of the new compounds were elucidated by mass spectrometry and NMR analysis, Supporting Information (S2-S9), whereas those of the previous reported analogues **4** [15], **5-8**, **10**, **12-14** [16], and **15** [21], were elucidated by comparison of their spectral data with those reported in the literature.

2.2. Biological evaluation

2.2.1. Anti-kinetoplastid activity

In an effort to identify more potent withanolides than withaferin A (WA, **1**), the *in vitro* inhibitory concentrations 50 (IC_{50}) of lead compound **1** and its analogues **2-15** (Fig. 1) was determined against different kinetoplast species. This value gives the concentration of the compound that eliminates the 50 % of the population of parasites. Promastigotes of *Leishmania amazonensis* and *L. donovani*, amastigotes of *L. amazonensis* and epimastigotes of *Trypanosoma cruzi* were used in this study. In addition, a mammalian cell line (murine macrophage J7741A.1) was used to test the cytotoxicity of the compounds. The selectivity index (SI) of the withanolides was calculated from the cytotoxic concentration 50 (CC_{50}) divided by the IC_{50}. In order to categorize the results, the compounds were classified according to the safety criteria described by Suffness [22], whose selectivity index value of two or more is considered as good selectivity. Miltefosine and benznidazole were used as reference drugs for anti-leishmanial and anti-trypanosomal activity, respectively (Table 1).

The results of *in vitro* assays against *L. amazonensis* promastigotes revealed that 9 analogues (compounds **2–6**, **8–10** and **12**) showed potent anti-leishmanial activity. These compounds showed higher inhibition than that of the widely known reference drug (miltefosine, IC_{50} 6.48 μM) with IC_{50} values ranging from 0.36 to 1.11 μM (Table 1). Furthermore, these compounds showed similar activity to the lead compound WA (**1**, IC_{50} 0.83 μM) (Table 1). All nine analogues showed a good selectivity index (SI), except for compound **4**, which had the highest cytotoxic activity.

In especial, compound **10** was 18 and 2.3 times more potent than miltefosine and WA (**1**), respectively.

Secondly, the anti-kinetoplastid activity on *L. donovani* promastigotes showed that four steroids (compounds **3**, **8**, **10** and **12**) exhibited potent anti-leishmanial activity. These compounds reached similar activity to miltefosine (IC_{50} 3.31 μM) with IC_{50} values ranging from 2.01 to

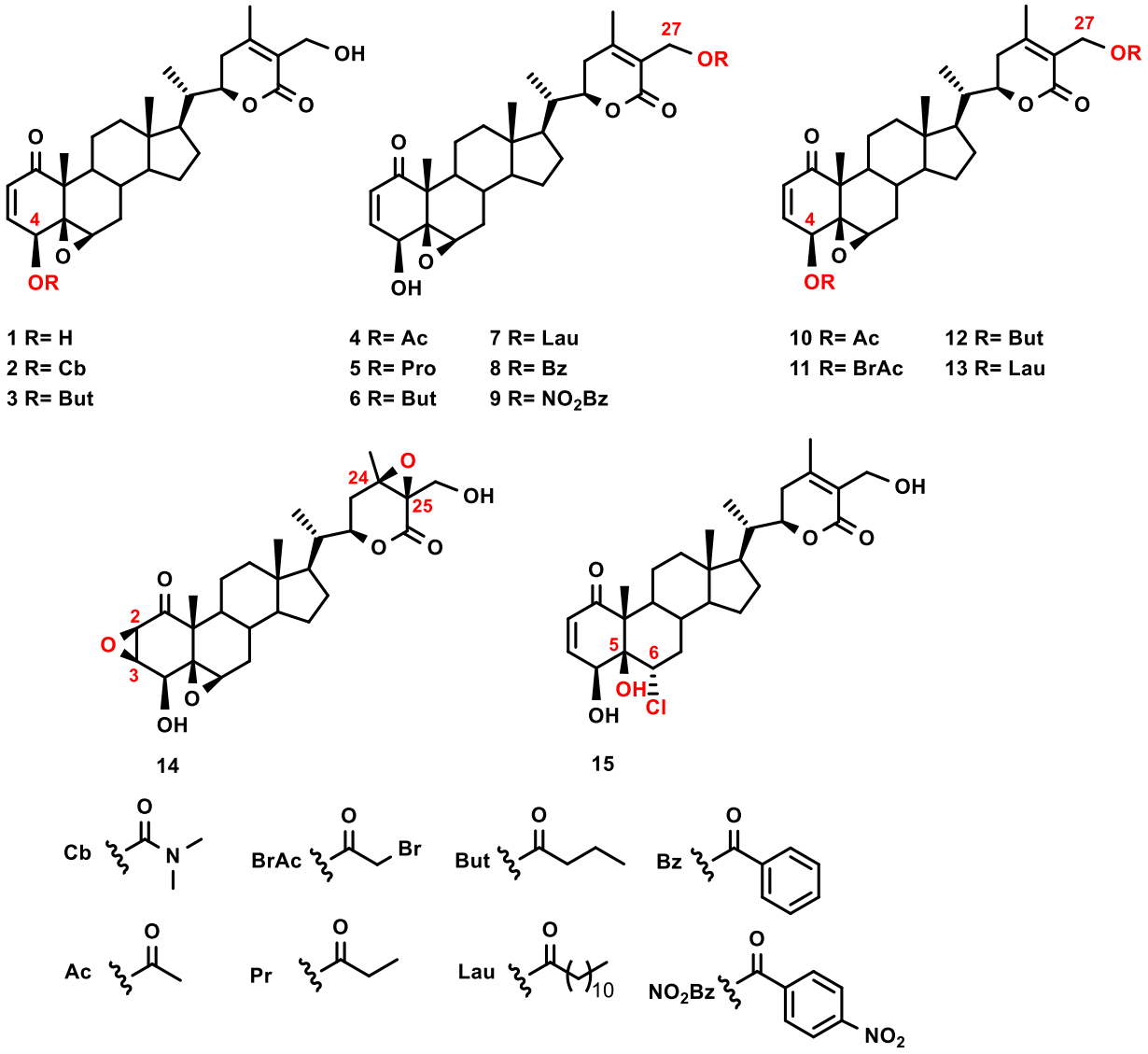

Fig. 1. Structure of withaferin A analogues (**2**-**15**).

3.18 μM (Table 1). In addition, seven analogues (compounds **2**, **3**, **5**, **6**, **8**, **10** and **12**) with IC_{50} values ranged from 2.01 to 6.82 μM, showed higher anti-kinetoplastid activity than the parent compound (WA, **1**, IC_{50} 13.22 μM) (Table 1). Unfortunately, they exhibited low selectivity index (SI≤1.0), which is a clear indication of non-selective effects, and therefore the analogues are toxic to *L. donovani* as well as to mammalian cell lines, except for compounds **3** (SI=2.3) and **10** (SI=2.0).

In our previous work, twenty-four known silyl ether derivatives of withaferin A showed potent activities against *L. amazonensis* promastigotes, which was similar to those obtained in the present work. One of them, 27-*tert*-butyldimethyl silyl ether WA (IC_{50} 0.19 μM, SI=65.3) was 34 times more active than miltefosine. Comparing this result with the fully acetylated derivative **10** (4,27-diacetylwithaferin A, IC_{50} 0.36, SI=15.6), which was 18 times more active than the reference drug, it appears that WA analogue based on silyl ethers exhibit little better anti-leishmanial activities. However, the silyl ether analogues of WA were not active against *L. donovani* promastigotes, whereas the present withasteroids showed promising anti-leishmanial activity against this *Leishmania* specie [23]. Moreover, the current results are agreement with earlier studies, which showed that several natural withanolides are promising anti-leishmanial agents, such as two withanolides from *Aurelia fasciculata*, Aurelianolide A and B (IC_{50} 7.61 μM and 7.94 μM, respectively) on *L. amazonensis* promastigotes [24], and withanolide J from *Withania coagulans* on *L. major* promastigotes (IC_{50} 5.70 μM) [25]. In both studies, the natural withanolides did not display better anti-leishmanial activity than the present WA analogues.

As a final point, the antiparasitic activity against *T. cruzi* epimastigotes revealed that nine withasteroids (compounds **2**-**6**, **8**-**10** and **12**) showed potent anti-trypanosomal activity with IC_{50} values ranging from 0.19 to 1.84 μM (Table 1). These analogues showed higher inhibition than the widely known reference drug (benznidazole, IC_{50} 6.95 μM). In addition, three compounds (**3**, **4** and **6**) showed similar activity to WA (**1**, IC_{50} 1.02 μM) and three analogues (**8**-**10**) higher than the lead compound (Table 1). All nine analogues showed a good selectivity index (SI), except compounds **4** and **12**, with values ranging from 3.0 to 30. Among them, once again analogue **10** showed the best biological profiles combining the experimental results of anti-kintoplastid activity and selectivity index. Thus, compound **10** was 36.6 and 5.4 times more potent than benznidazole and WA (**1**), respectively. In our previous work, the silyl ether analogues of WA presented an anti-trypanosomal activity similar to that obtained by the present work [23], where the 27-*tert*-butyldimethyl silyl ether WA analogue (IC_{50} 0.14 μM, SI=88.6) stood out for being 49 times more active than benznidazole. This result of anti-trypanosomal activity was similar to

Table 1
Anti-kinetoplastid activity of withanolides **1–15** against the promastigote stage of *Leismania spp*, epimastigote stage of *T. cruzi* and cytotoxicity against mammalian cells (IC_{50} and CC_{50} expressed in μM).

Compds	*L. amazonensis*		*L. donovani*		*T. cruzi*		*J774A.1*
	IC_{50}^{a}	SI[c]	IC_{50}^{a}	SI[c]	IC_{50}^{a}	SI[c]	CC_{50}^{b}
1	0.83 ± 0.07	14.4	13.22 ± 1.16	0.9	1.02 ± 0.10	11.7	11.92 ± 1.08
2	1.11 ± 0.13	5.1	6.35 ± 0.86	0.9	1.84 ± 0.06	3.0	5.59 ± 0.28
3	0.84 ± 0.03	5.5	2.01 ± 0.38	2.3	1.22 ± 0.08	3.8	4.69 ± 0.06
4	0.60 ± 0.01	1.4	24.01 ± 0.86	0.0	0.73 ± 0.07	1.1	0.82 ± 0.04
5	0.99 ± 0.18	5.2	6.61 ± 0.89	0.8	1.72 ± 0.15	3.0	5.23 ± 0.06
6	0.76 ± 0.03	6.9	6.82 ± 0.76	0.8	0.83 ± 0.09	6.4	5.30 ± 0.02
7	8.60 ± 0.11	2.8	> 50.00		16.30 ± 3.52	1.5	24.03 ± 2.82
8	0.58 ± 0.02	3.1	3.18 ± 0.16	0.6	0.38 ± 0.09	4.7	1.79 ± 0.13
9	0.49 ± 0.04	4.7	9.11 ± 0.09	0.2	0.28 ± 0.06	8.1	2.31 ± 0.08
10	0.36 ± 0.02	15.6	2.82 ± 0.09	2.0	0.19 ± 0.03	30.0	5.59 ± 0.28
11	35.99 ± 2.40	2.0	> 50.00		> 50.00		72.37 ± 1.30
12	0.64 ± 0.05	4.7	2.09 ± 0.17	1.4	1.78 ± 0.29	1.7	3.00 ± 0.42
15	8.33 ± 0.31	4.7	> 50.00		12.18 ± 0.59	3.2	39.39 ± 2.89
M[d]	6.48 ± 0.10	11.1	3.31 ± 0.11	21.8			72.18 ± 1.25
B[d]					6.95 ± 0.50	57.5	399.91 ± 1.04

[a] IC_{50}: concentrations able to inhibit 50 % of parasites after 72 h, expressed as μM ± standard deviation (SD). [b] CC_{50} concentration able to inhibit 50 % of murine macrophages after 24 h, expressed as μM ± standard deviation (SD). [c]SI: selectivity index (CC_{50}/IC_{50}). [d] M: Miltefosine was used as positive control against *L. amazonensis* and *L. donovani*. [d] B: Benznidazole was used as positive control against *T. cruzi*. Anti-kinetoplastid activity and cytotoxicity assays were performed as independent experiments in triplicates. Analogues 13 and 14 were excluded due to their low antiparasitic activity (data not shown).

that obtained with the 4,27-diacetylwithaferin A (withasteroid **10**) of the present study, in which this compound was 36.6 times more active than this reference drug.

These anti-trypanosomal data are agreement with previous report, and confirm the withanolides as a promising scaffold. In this sense, Aurelianolide A (IC_{50} 5.68 μM) and B (IC_{50} 5.72 μM) from *Aureliana fasciculata* var. *fasciculata* [26], and Physagulin C (IC_{50}, 14 μM) from *Physalis angulate* [27] showed potent activity in *T. cruzi* epimastigotes. In both studies, the withanolides have not shown a better antikinetoplastid profile than the withanolides from the present structural modification of WA (**1**).

Overall, looking at the literature data mentioned above, it appears that for both *Leishmania* spp. and *T. cruzi*, the synthesis of WA analogues has optimised and improved the anti-leishmanial and anti-trypanosomal activity of WA. Based on the *in vitro* results on *Leishmania* spp promastigotes, analogues **2**, **3**, **5-7**, **10** and **11** were selected for further studies on the intracellular amastigote stage of *L. amazonensis* (Table 2). Their anti-leishmanial activity showed that all withanolides, except steroid **11**, were more potent than miltefosine (IC_{50} 3.12 μM) with IC_{50} values ranging from 0.36 to 1.77 μM. These compounds were between 1.8 and 8.7 times more potent than the reference drug. Moreover, all of them were less active than the lead compound (WA, **1**) and showed a good selectivity index with values ranging from 3.9 to 14.4. According to the literature, there are some previous research that studied the anti-leishmanial activity of withanolides against the intracellular form of

Table 2
Anti-leishmanial activity of withanolides **1-3**, **5-7** and **10–11** against the amastigote stage of *L. amazonensis*, and cytotoxicity against mammalian cells (IC_{50} and CC_{50} expressed in μM).

Compds	*L. amazonensis*		*J774A.1*
	IC_{50}^{a}	SI[c]	CC_{50}^{b}
1	0.06 ± 0.01	198.7	11.92 ± 1.08
2	0.95 ± 0.04	5.9	5.59 ± 0.28
3	1.21 ± 0.27	3.9	4.69 ± 0.06
5	0.36 ± 0.05	14.4	5.23 ± 0.06
6	0.41 ± 0.02	12.8	5.30 ± 0.02
7	1.77 ± 0.05	13.6	24.03 ± 2.82
10	0.50 ± 0.03	11.2	5.59 ± 0.28
11	11.20 ± 2.00	6.4	72.37 ± 1.30
M[d]	3.12 ± 0.12	23.13	72.18 ± 1.25

[a] IC_{50}: concentrations able to inhibit 50 % of parasites after 24 h, expressed as μM ± standard deviation (SD). [b] CC_{50} concentration able to inhibit 50 % of murine macrophages, expressed as μM ± standard deviation (SD). [c] SI: electivity index (CC_{50}/IC_{50}). [d] M: Miltefosine was used as the positive control against *L. amazonensis*. Anti-kinetoplastid activity and cytotoxicity assays were performed as independent experiments in triplicates.

Leishmania spp. In our previous search on silyl ether analogues of WA, the synthetized analogues showed similar activity on *L. amazonensis* amastigotes (IC_{50} values ranging from 0.12 to 0.80 μM) to that reported in the present study for withasteroids (IC_{50} values ranging from 0.36 to 1.77 μM) [23]. In none of the cases, withanolides synthesised from WA improved the activity presented by this natural molecule in *L. amazonensis* amastigotes. On the other hand, natural withanolides Aurelianolide A (IC_{50} 2.25 μM) and B (IC_{50} 6.43 μM) on *L. amazonensis* amastigotes [24], showed activities lower than the withanolides reported in the present study. Therefore, the synthesis of withanolides from WA based on silicon ethers or esters did not improve the anti-leishmanial activity against *L. amazonensis* amastigotes but does not seem to exceed in any case the activity of WA (**1**).

On the other hand, based on the anti-trypanosomal activity results, analogues **6**, **9** and **10** were selected to determine their activity against the amastigote stage of *T. cruzi* (Table 3). Their anti-trypanosomal activity showed that all withanolides were more potent than benznidazole (IC_{50} 2.67 μM), with IC_{50} values ranging from 0.70 to 1.08 μM. These compounds were 2.47–3.8 times more potent than the reference drug. Although all analogues were less selective than the reference drug, they showed a good selectivity index with values ranging from 2.1 to 7.5. It is noteworthy that these are the first results on the activity of withanolides against the intracellular form of *T. cruzi*, because there are no reports in the literature on the activity of withanolides or their synthetic analogues on *T. cruzi* amastigotes.

2.2.2. Structure-activity relationship studies

The influence of the substitution pattern on the susceptibility of

Table 3
Anti-trypanosomal activity of withanolides **6, 9** and **10** against the amastigote stage of *T. cruzi*, and cytotoxicity against mammalian cells (IC_{50} and CC_{50} expressed in μM).

Compds	*T. cruzi*		*J774A.1*
	IC_{50}^{a}	SI[c]	CC_{50}^{b}
6	0.70 ± 0.04	7.5	5.30 ± 0.02
9	1.08 ± 0.11	2.1	2.31 ± 0.08
10	1.03 ± 0.20	5.4	5.59 ± 0.28
B[d]	2.67 ± 0.39	149.8	399.91 ± 1.04

[a] IC_{50}: concentrations able to inhibit 50 % of parasites after 24 h, expressed as μM ± standard deviation (SD). [b] CC_{50} concentration able to inhibit 50 % of murine macrophages, expressed as μM ± standard deviation (SD). [c] SI: electivity index (CC_{50}/IC_{50}). [d] B: Benznidazole was used as the positive control against *T. cruzi*. Anti-kinetoplastid activity and cytotoxicity assays were performed as independent experiments in triplicates.

kinetoplastids to the WA analogues studied in this work (**2**-**15**) was carried out taking into consideration the IC_{50} values against the lines assayed, WA has been included to broaden the SAR analysis, and for comparative purposes, revealing the followings trends of the structure-activity relationship.

To explore the SAR, we started our effort to study the role of the ester groups at C-4 and C-27 on the activity. Thus, comparison of the activity of the three groups of ester analogues, the 4-ester (**2**, and **3**), 27-ester (**4**-**9**) and the 4,27-diester (**10**-**13**) withanolides with their congenere, WA (Scheme 1, Table 1), showed that the esterification of hydroxyls did not enhance the anti-kinetoplastid activity against *L. amazonensis* promastigotes and *T. cruzi* epimastigotes with respect to the lead compound. However, the acylation increased the potency on *L. donovani* promastigotes. But, unfortunately this enhance in leishmanicidal potency was not accomplished by the therapeutic ratio. These data suggesting such differences in the potency and selectivity index depend a great extent on the parasite strain tested.

Moreover, the physicochemical properties of the substitution patterns from the acyl chain lead to a broad range of potency and selectivity index in each of the four parasites strain, overall, these findings suggested that acylation of hydroxyl groups at the C-4/C-27 positions fine tune the antikinetoplastid profile of this type of steroids.

The influence of functional groups on the A, B and lactone rings was evident in all strains assayed, comparing the antiparasitic activity of WA with those of analogues **14** and **15**, as simple modification of double bond at C-2(3) and C-24(25) (**14** vs **1**) or epoxy group at C-5(6) (**15** vs **1**) produced a dramatic loss of antikinetoplastid activity.

These results showed that the α,β-unsaturated ketone on ring A, the 5β,6β-epoxide in ring B, and the side-chain with an α,β-unsaturated *δ*-lactone group, are relevant groups on the steroids skeleton that interact with the receptor and appears to be the functional groups of the molecule responsible for the anti-kinetoplastid activity and therefore could be part of the structural features requirements or pharmacophore. While the acylation of hydroxyl groups seem to modify the activity and therefore these would form part of the auxophore, since the potency and therapeutic index largely depending on the physiochemical properties of the type of ester.

2.2.3. Study on the mechanism of action

Considering the *in vitro* antikinetoplastid activity on *Leishmania* spp. promastigotes, *L. amazonensis* amastigotes, *T. cruzi* epimastigotes and amastigotes and cytotoxicity on murine J7741A.1. macrophages, some compounds were selected for further studies in order to elucidate the mechanism of action of the compounds in the parasites and whether they induce programmed cell death or other mechanism of death like necrosis or autophagy. Compounds **5**, **6**, **7** and **10** were tested on promastigotes stage of *L. amazonensis*; compounds **3** and **10** on *L. donovani* promastigotes; and compounds **6**, **9** and **10** on epimastigotes of *T. cruzi*.

First, Trypanosomatids are parasites with a single mitochondrion, thus this organelle is one of the main targets for drug discovery and development new therapeutic agents. To analysis the mitochondrial ATP levels on the parasites, the promastigotes of *Leishmania* spp. and epimastigotes of *T. cruzi* were incubated with the IC_{90} of the analogues (**3**, **5–7**, **9** and**10**). The results are represented for *L. amazonensis* and *L. donovani* (Fig. 2) and for *T. cruzi* (Fig. 3), as the percentage of inhibition of ATP levels compared to the control, which represents the 100 % of ATP. The levels analysis showed a significant decrease in values against all three parasites tested, which was more than 50 % compared to the untreated parasites. Moreover, this underlying mechanism highlighting the diacetyl derivative **10** against *L. amazonensis* promastigotes, which caused a significant decrease of mitochondrial ATP levels, with reduction value of 99 % in compared to the control.

Second, the mitochondrial membrane potential analysis on *Leishmania* spp promastigotes (Fig. 4), and *T. cruzi* epimastigotes (Fig. 5), showed that selected withanolides (**3**, **5–7**, **9** and **10**) produce a significant decrease in mitochondrial membrane potential against parasites of

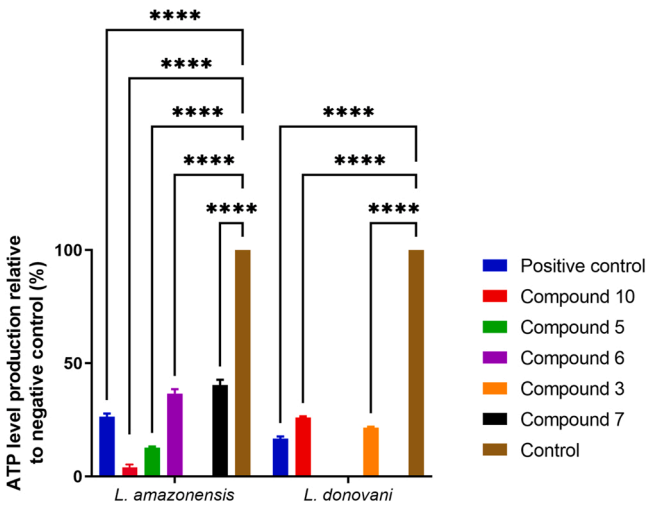

Fig. 2. ATP level (%) in promastigotes of *L. amazonensis* and *L. donovani* incubated with IC_{90} of the compounds relative to negative control. Sodium azide 20 mM was used as a positive control. A negative control consisting of untreated parasites was also added as a reference for normal conditions in cellular ATP levels. The assays were performed as independent experiments in triplicates. Analysis of variance was determined by one-way ANOVA using GraphPad.PRISM® 9.0 software. Significance differences when comparing different percentages values are represented like ns = non-significant; *p < 0.1; ** p < 0.01; *** p < 0.001 and **** p < 0.0001.

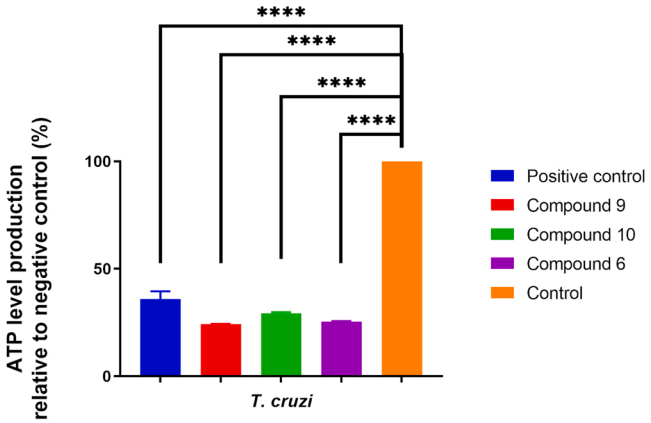

Fig. 3. ATP level (%) in epimastigotes of *T. cruzi* incubated with IC_{90} of the compounds relative to negative control. Sodium azide 20 mM was used as a positive control. A negative control consisting of untreated parasites was also added as a reference for normal conditions in cellular ATP levels. The assays were performed as independent experiments in triplicates. Analysis of variance was determined by one-way ANOVA using GraphPad.PRISM® 9.0 software. Significance differences when comparing different percentages values are represented like ns = non-significant; *p < 0.1; ** p < 0.01; *** p < 0.001 and **** p < 0.0001.

L. amazonensis and *L. donovani*. In the case of *L. amazonensis*, there was a more pronounced decrease in mitochondrial membrane potential, which was reduced by approximately 96 % after incubation with all compounds tested against this parasite. On the other hand, unexpected opposite results were observed for *T. cruzi*, where the analogues (**6**, **9** and **10**) caused a significant increase in mitochondrial membrane potential compared to the control.

Third, to assess whether WA analogues (**3**, **5-7**, **9** and**10**) induce alterations in the permeability of the cytoplasmic membrane of the parasites, they were incubated for 24 h with the IC_{90} of the different steroids and analyzed using SYTOX® Green dye as fluorescence. The results on *L. amazonensis* (Fig. 6), *L. donovani* (Fig. 7) and *T. cruzi*

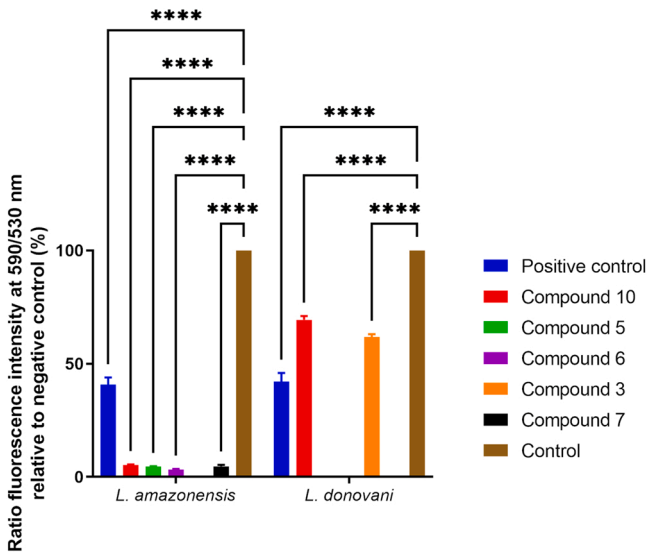

Fig. 4. Percentage relative to the negative control of the fluorescence intensity ratio at 590/530 nm in promastigotes of *L. amazonensis* and *L. donovani* incubated with IC_{90} of the compounds. 100 μM CCP was used as a positive control. A negative control consisting of untreated parasites was also added as a reference for normal mitochondrial membrane potential conditions. The assays were performed as independent experiments in triplicates. Analysis of variance was determined by one-way ANOVA using GraphPad.PRISM® 9.0 software. Significance differences when comparing different percentages values are represented like NS non-significant; *p < 0.1; ** p < 0.01; *** p < 0.001 and **** p < 0.0001.

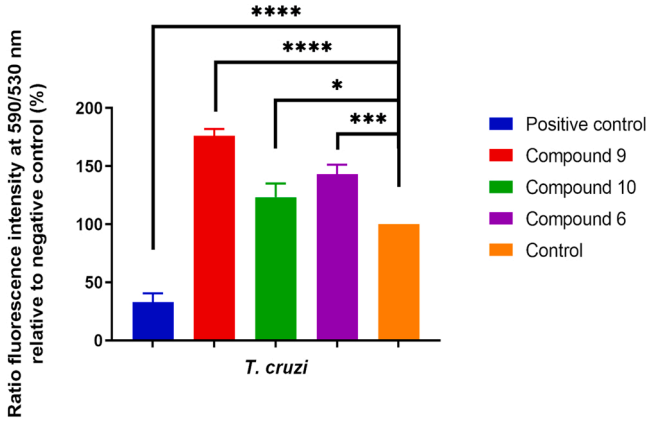

Fig. 5. Percentage relative to the negative control of the fluorescence intensity ratio at 590/530 nm in epimastigotes of *T. cruzi* incubated with IC_{90} of the compounds. 100 μM CCP was used as a positive control. A negative control consisting of untreated parasites was also added as a reference for normal mitochondrial membrane potential conditions. The assays were performed as independent experiments in triplicates. Analysis of variance was determined by one-way ANOVA using GraphPad.PRISM® 9.0 software. Significance differences when comparing different percentages values are represented like NS non-significant; *p < 0.1; ** p < 0.01; *** p < 0.001 and **** p < 0.0001.

(Fig. 8), showed that only withanolide **10** against *L. amazonensis* induced increased the plasmatic membrane permeability of the parasite, since a clear green fluorescence could be observed. However, as can be seen under transmitted light, the integrity and cellular shape of the parasite was maintained, ruling out a process of cell death due to necrosis [14]. While the rest of the WA derivatives did not induce any change in the permeability of the cytoplasmic membrane against the three parasites tested.

Forth, chromatin condensation is one of the most characteristic

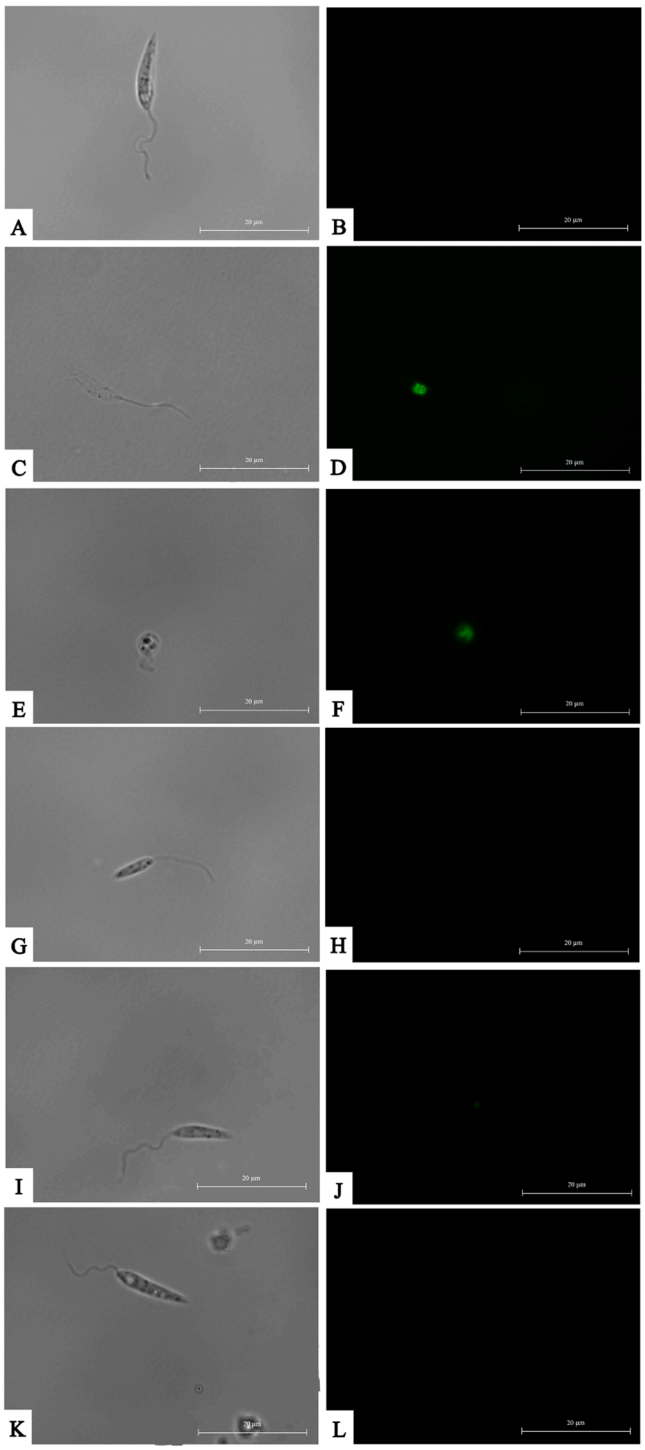

Fig. 6. Analysis of plasma membrane permeability of *L. amazonensis* promastigotes. Negative control of *L. amazonensis* promastigotes without any treatment (A, B), positive control of *L. amazonensis* promastigotes incubated with Triton X-100 at a concentration of 0.1 % for 30 min (C, D), promastigotes incubated with IC_{90} of withanolide **10** (E, F), withanolide **5** (G, H), withanolide **6** (I, J) and withanolide **7** (K, L) during 24 h. The 100X images were captured using an EVOS® FL Cell Imaging System. Scale-bar: 20 μm. The assays were performed as independent experiments in triplicates.

signals of apoptotic cell death [28]. The analysis was made by Hoechst 33342 reagent, which binds to the condensed DNA of the parasite and emits blue fluorescence, and propidium iodide binds to the DNA of dead parasites and emits red fluorescence, thus evidencing an advanced

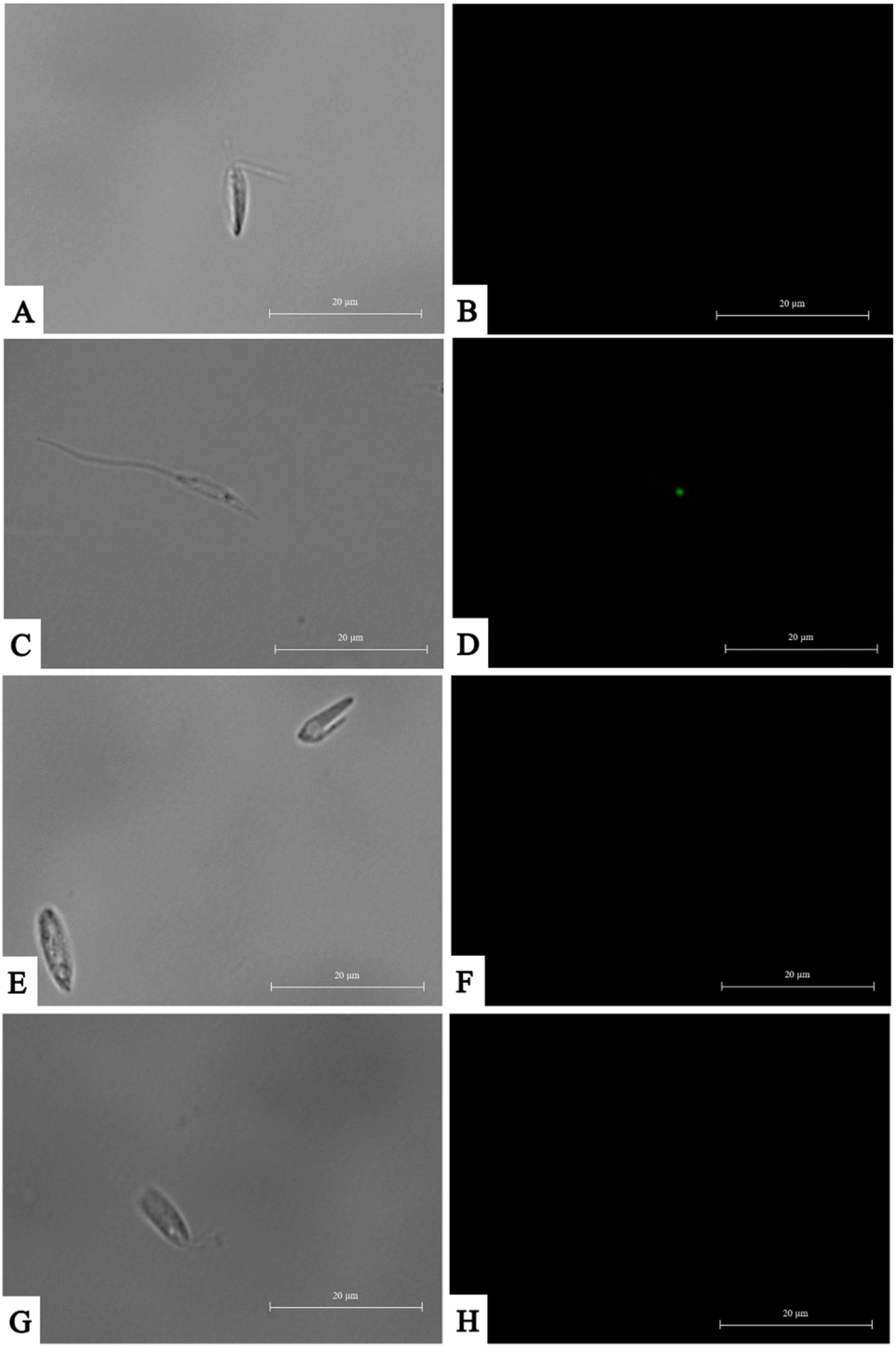

Fig. 7. Analysis of plasma membrane permeability of *L. donovani* promastigotes. Negative control of *L. donovani* promastigotes without any treatment (A, B), positive control of *L. donovani* promastigotes incubated with Triton X-100 at a concentration of 0.1 % for 30 min (C, D), promastigotes incubated with IC_{90} withanolide **10** (E, F) and withanolide **3** (G, H) during 24 h. The 100X images were captured using an EVOS® FL Cell Imaging System. Scale-bar: 20 µm. The assays were performed as independent experiments in triplicates.

process of death. The results against *L. amazonensis* (Fig. 9), *L. donovani* (Fig. 10) and *T. cruzi* (Fig. 11) exhibited a clear chromatin condensation in all the parasites incubated with these steroids (**3**, **5–7**, **9** and **10**), they showed intense blue fluorescence inside the nucleus. Moreover, no red fluorescence was observed, so it could be deduced that a process compatible to early apoptosis is being induced in the parasites. Withanolide **10** stands out, since a red fluorescence was observed as well in *L. amazonensis*, indicating an advanced process of death, compatible to a late apoptosis in this case.

Fifth, another well-known physiological change that induces programmed cell death on eukaryotic cells is the intracellular accumulation of reactive oxygen species (ROS) [29]. The analysis was carried out by CellROX® deep red reagent, and the accumulation of ROS is measured by the fluorescence emission in the red spectral range inside the cells. All parasites *L. amazonensis* (Fig. 12), *L. donovani* (Fig. 13) and *T. cruzi* (Fig. 14) showed an intense red fluorescence after being incubated with the analogues, thus evidencing a clear accumulation of ROS inside parasites, which causing a poor growth of parasites.

Finally, autophagy, another type of programmed cell death that can occur in some parasites and has recently been investigated in kinetoplasts like *Leishmania* is autophagy [30]. In this way, this programmed cell death study was carried out using monodansylcadaverine dye,

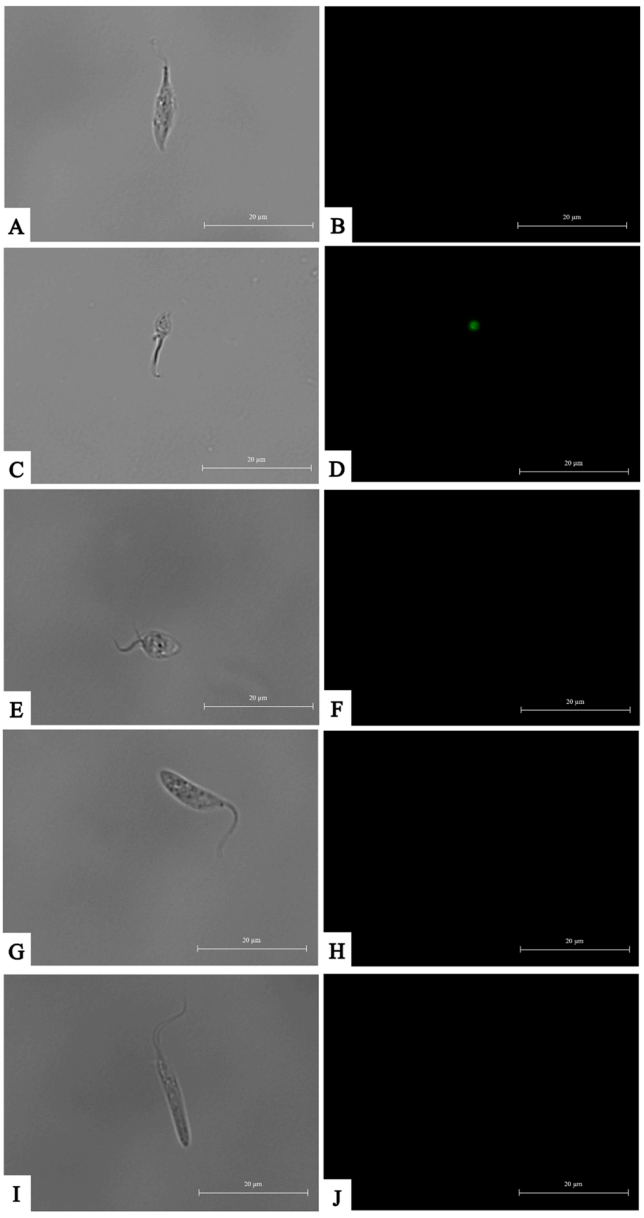

Fig. 8. Analysis of plasma membrane permeability of *T. cruzi* epimastigotes. Negative control of *T. cruzi* epimastigotes without any treatment (A, B), positive control of *T. cruzi* epimastigotes incubated with Triton X-100 at a concentration of 0.1 % for 30 min (C, D), epimastigotes incubated with IC_{90} of withanolide **9** (C, D), withanolide **10** (E, F) and withanolide **6** (G, H) during 24 h. The 100X images were captured using an EVOS® FL Cell Imaging System. Scale-bar: 20 μm. The assays were performed as independent experiments in triplicates.

which showed a characteristic autophagic vacuoles with an intense blue fluorescence. The tested withanolides induced the formation of autophagic vacuoles in all parasites on *L. amazonensis* (Fig. 15), *L. donovani* (Fig. 16) and *T. cruzi*, (Fig. 17), except for withanolide **3** in *L. donovani*. As shown, the small accumulations of blue fluorescence are evident and correspond to the expected size of small autophagic vesicles (white arrows in Figures).

These advanced biological experiments to explore their mechanism of action showed that withasteroids synthesized from WA induced apoptosis-like death in promastigotes of *L. amazonensis*, *L. donovani* and epimastigotes of *T. cruzi*, they are able to cause decreased cellular ATP levels, alterations in mitochondrial membrane potential, chromatin condensation and increased intracellular ROS levels, which are cellular events compatible with apoptosis that have been previously reported in the literature [31,32]. There are different studies on the apoptosis-inducing capacity of WA, as well as of natural withanolides or synthetic WA analogues, in different cellular organisms. In this sense, WA has been reported to be a molecule with potent antineoplastic capacity by the induction of apoptosis in cancer cells and in experimental animal models with glioblastomas, dermatological diseases, and breast cancer [17,33,34]. Furthermore, this type of programmed cell death has also been observed in *Leishmania* spp. parasites through ROS formation, mitochondrial alterations and chromatin condensation [11,18]. Previous work has reported that WA inhibits protein kinase C (important in apoptosis signalling pathways) in *L. donovani*, causing depolarisation of the mitochondrial membrane potential, generating ROS inside the parasites and inducing DNA fragmentation. Finally, these events induced apoptosis-like cell death of the parasite [35,36]. Moreover, natural withanolides isolated from *Withania somnifera* induced apoptotic-like death in *L. donovani* promastigotes via production of ROS and disruption of mitochondrial membrane potential [37]. These cellular events characteristics of an apoptosis-like mechanism have also been reported with withanolides synthesised from WA [23], after incubating *L. amazonensis* promasitoges and *T. cruzi* epimastigotes with silyl ether analogues of WA, the cellular events compatible with apoptosis reported in this work were also observed: decrease in ATP levels, alterations of the mitochondrial membrane potential, chromatin condensation and ROS formation. Therefore, all these studies reinforce the results obtained in the present work and the promising capacity of withanolides, not only natural but also synthetic WA analogues, as inducers of apoptosis-like cell death in tripanosomatids. On the other hand, the withasteroids of the present study induced the formation of autophagic vacuoles in all the parasites tested, except for withanolide **3** in *L. donovani*. It became evident that these withasteroids were able to activate two types of programmed cell death in tripanosomatids: apoptosis-like and autophagy. These results can be related to research carried out in colorectal cancer cells, in which the WA could stimulate activation of both apoptosis and autophagy process via modulating β-catenin pathway in these cancer cells [38]. Moreover, the present results are agreement with previous work [23] carried out with WA-silyl ether analogues, wherein, all selected withanolides induced apoptosis-like death and autophagy vacuole formation in *L. amazonensis* and *T. cruzi*. On the other hand, in a recent review which is focused on drugs that initially induce autophagy and then turning into apoptosis-like cell death of parasites, cryptolepine generated MCD-positive autophagy vacuoles in *L. donovani* and subsequently different apoptosis-like events, such as DNA fragmentation [39]. These studies and the present results suggest as the main hypothesis would be that at low doses of withasteroids **3**, **5**, **6**, **7**, **9**, **10** autophagy is initially activated as a survival mechanism in trypanosomatids, however, if these unfavorable conditions for the parasites continue, the parasites may activate an apoptotic type of cell death.

In summary, withasteroids represent a wide range of therapeutic possibilities against Chagas disease and leishmaniasis, promising to update and improve current lines of treatment.

3. Conclusion

Withaferin A (WA), a natural product of whitanolide-type steroid, was identified as an effective anti-kinetoplastid agents in our previous research. In this study, according to rational drug design strategy, a total of 14 derivatives were designed, synthesized, and biological evaluation after a preliminary structure-based optimization of WA. Antiparasitic results against strain of *Leishmania* spp and *T.cruzi* showed that nine WA derivatives exhibited potent activities, at the sub-micromolar level with a good selectivity index, close to WA and better than that of reference drugs, miltefosine and benznidazole. Oustanding analogue **10** (4,27-diacetylwithaferin A), the most potent, showing an 18 and 36-fold greater effectiveness antikinetoplastid activity than reference drugs. Moreover, through SAR analysis, the α,β-unsaturated ketone, epoxide

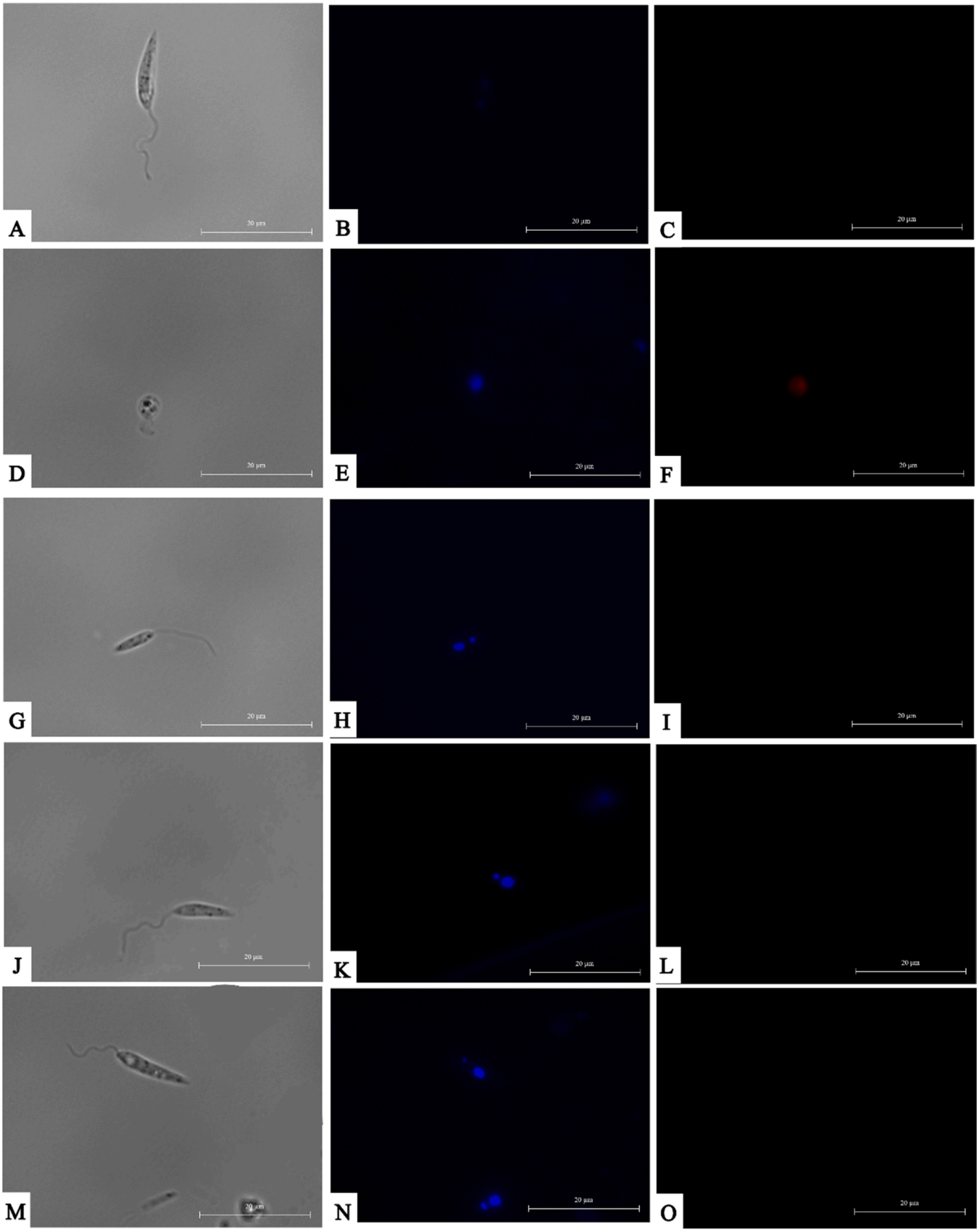

Fig. 9. Chromatin condensation determination of *L. amazonensis* promastigotes. Negative control of *L. amazonensis* promastigotes without any treatment (A, B, C), promastigotes incubated with IC_{90} of withanolide **10** (D, E, F), withanolide **5** (G, H, I), withanolide **6** (J, K, L) and withanolide **7** (M, N, O) during 24 h. The 100X images were captured using an EVOS® FL Cell Imaging System. Scale-bar: 20 μm. The assays were performed as independent experiments in triplicates.

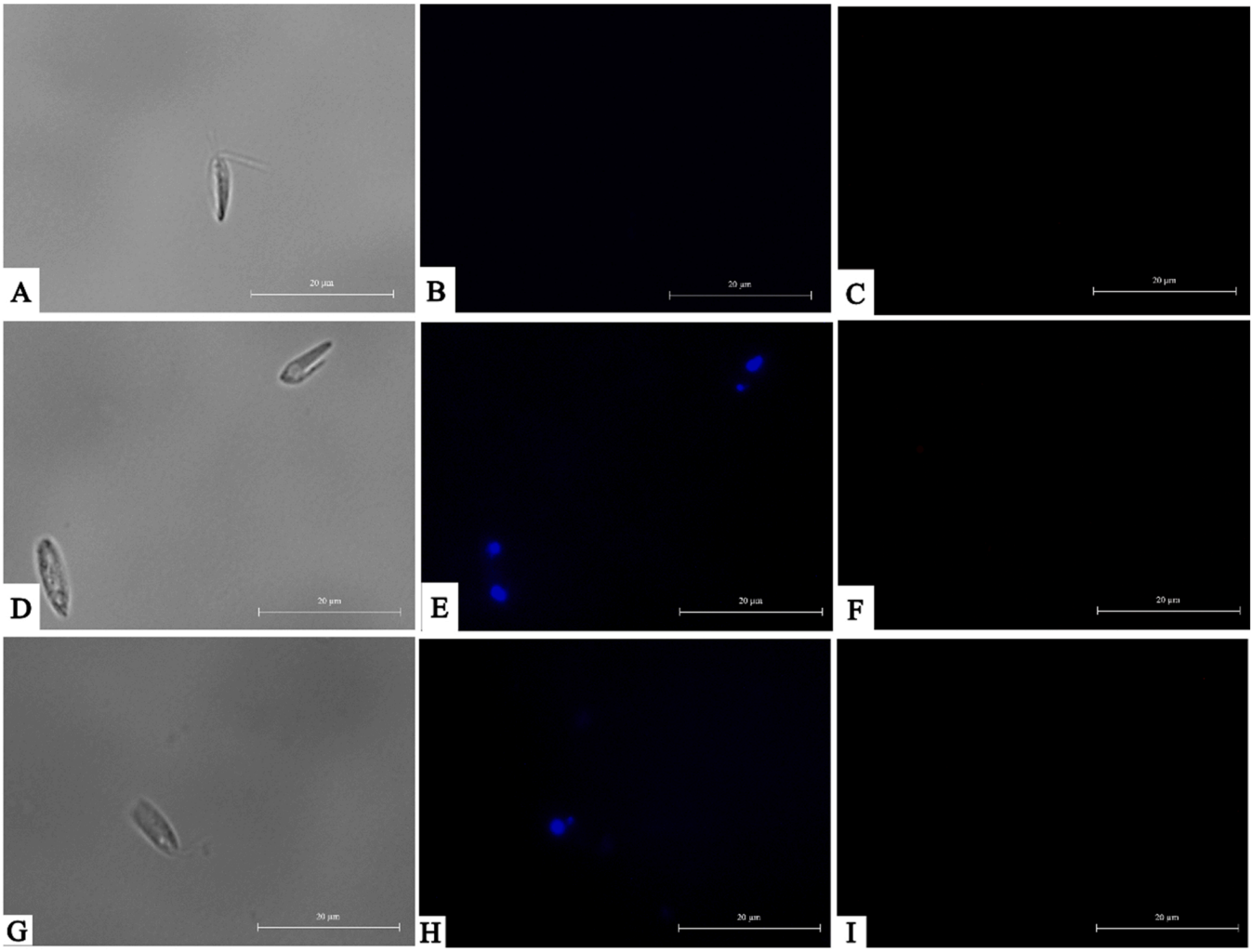

Fig. 10. Chromatin condensation determination of *L. donovani* promastigotes. Negative control of *L. donovani* promastigotes without any treatment (A, B, C), promastigotes incubated with IC_{90} withanolide **10** (D, E, F) and withanolide **3** (G, H, I) during 24 h. The 100X images were captured using an EVOS® FL Cell Imaging System. Scale-bar: 20 μm. The assays were performed as independent experiments in triplicates.

moiety and type of ester on the withasteroids skeleton play crucial role for the antiparasitic activity. Furthermore, the mechanism of action of selected compounds revealed that all compounds induce programmed cell death through a process of apoptosis-like by alterations in ATP levels, mitochondrial membrane potential, condensation of the chromatin and increase in reactive oxygen species and autophagy. All these findings showed that withanolide as a promising scaffold for synthesis of novel antimicrobial agents and could serve as a guide to development new agents and meaningful to kinetoplastid therapy in the future.

4. Material and methods

4.1. Chemistry

4.1.1. General methods

Optical rotations were measured on a Perkin Elmer 241 automatic polarimeter, in $CHCl_3$ at 25 °C, the $[\alpha]_D$ values are given in units of 10^{-1} deg cm^2 g^{-1}. 1D and 2D spectra were recorded on a Bruker Avance 400, 500 and 600 spectrometers; the chemical shifts are given in δ (ppm), coupling constants in Hz, and were referenced to the residual deuterated solvent ($CDCl_3$: δ_H 7.26, δ_C 77.16) with TMS as internal reference. EIMS and HREIMS were measured on a Micromass Autospec spectrometer, and ESIMS and HRESIMS (positive mode) were measured on a LCT Premier XE Micromass Autospec spectrometer. Silica gel 60 for column chromatography (particle size 15–40 and 63–200 μm), Polygram Sil G/UV_{254} used for analytical and preparative TLC, and HPTLC-Platten Nano-Sil 20 UV_{254} were purchased from Macherey-Nagel. Reactions were monitored by TLC; the spots were visualized by UV light and heating silica gel plates sprayed with H_2O-H_2SO_4-AcOH (1:4:20). Unless otherwise noted, solvents and reagents were obtained from commercial suppliers and used without further purification. Anhydrous THF and Cl_2CH_2 were distilled from sodium/benzophenone and calcium hydride ketyl under nitrogen, respectively. All solvents used were analytical grade from Panreac, and the reagents were purchased from Sigma Aldrich. Withaferin A (WA, **1**), used as starting material, was isolated from the leaves of *Withania aristata* as previously described.[1].

4.1.2. Analogues synthesis

Among the analogues, three out of fifteen are described for the first time: derivatives **2**, **3**, **9** and **11**. The new compounds were synthesized through the following protocol, Supporting Information (S1-S8), whereas those of the previous reported analogues were prepared according to our established protocol (EJMC-17).

4.1.3. General procedure for Acylation of 1

A solution of **1** (20–40 mg), dry triethylamine (0.1–0.2 mL) and an excess of the corresponding carboxylic acid derivative in dry CH_2Cl_2 (2 mL) was stirred under different sets of conditions, which are specified

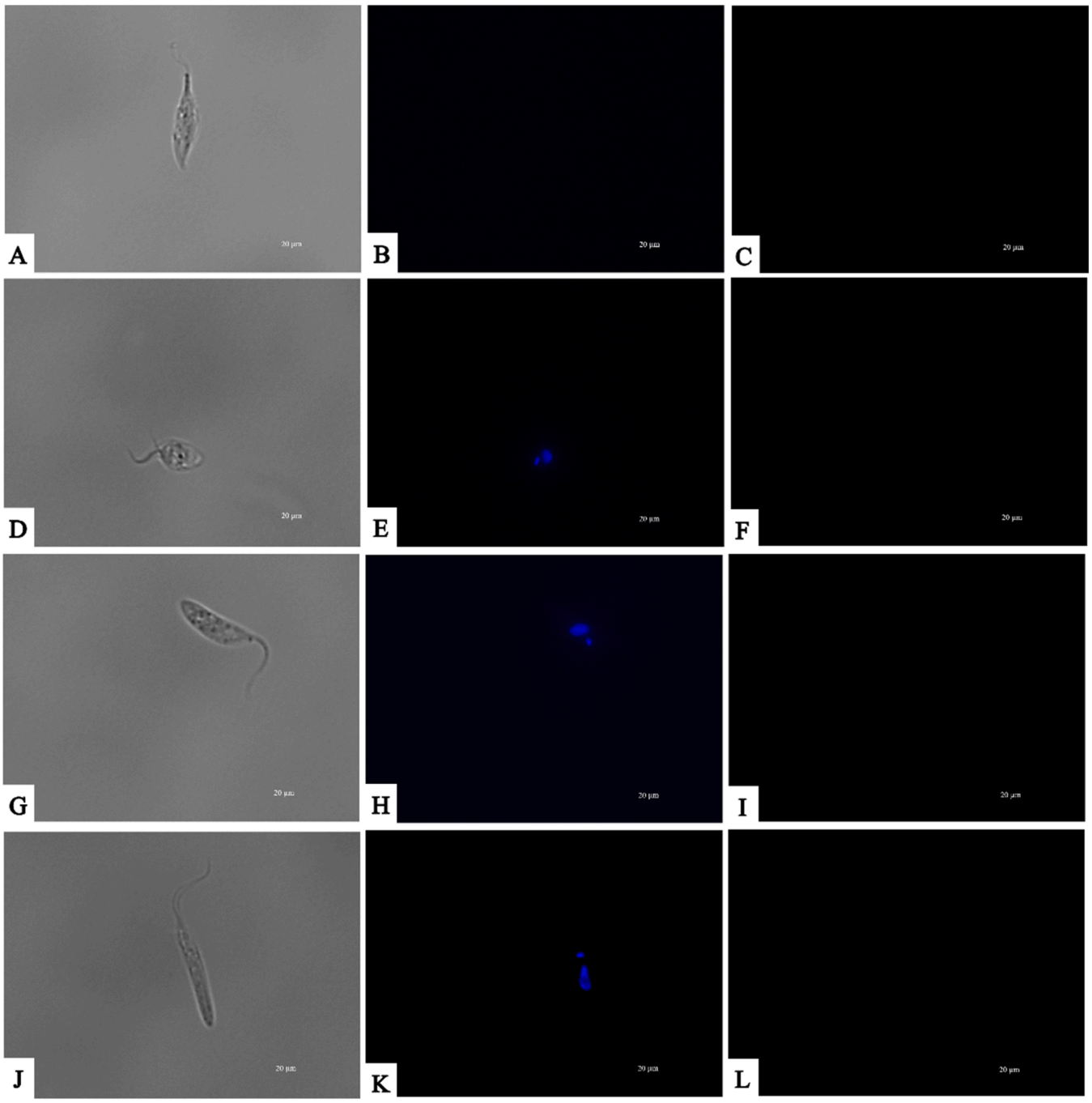

Fig. 11. Chromatin condensation determination of *T. cruzi* epimastigotes. Negative control of *T. cruzi* epimastigotes without any treatment (A, B, C), epimastigotes incubated with IC_{90} of withanolide **9** (D, E, F), withanolide **10** (G, H, I) and withanolide **6** (J, K, L) during 24 h. The 100X images were captured using an EVOS® FL Cell Imaging System. Scale-bar: 20 μm. The assays were performed as independent experiments in triplicates.

below for each procedure. The progress of the reaction was monitored by TLC using CH_2Cl_2/acetone (9/1). After the mixture was concentrated to dryness under reduced pressure, the residue was purified by preparative-TLC using CH_2Cl_2/acetone (9/1) to afford the corresponding esters (**2**-**11**). (EJMC-2017).

4.1.4. Preparation of derivative 2

To a solution of **1** (14 mg, 0.03 mmol), carbamoyl chloride (10 μl, 0.09 mmol) was added and stirred at room temperature for 48 h. The residue was purified yielding compounds **2** (8.8 mg, 54 %).

4-O-Dimethylcarbamoylwithaferin A (**2**). $[\alpha]_D^{25} = +120.0$ (*c* 0.80, $CHCl_3$); ^{1}H NMR (400 MHz, $CDCl_3$) δ 0.72 (3 H, s, Me18), 0.96 (1 H, m, H9), 0.98 (1 H, m, H14), 1.02 (3 H, d, $J = 6.6$ Hz, Me21), 1.10 (1 H, m, H12), 1.12 (1 H, m, H17), 1.19 (1 H, m, H15), 1.40 (1 H, m, H16), 1.41 (3 H, s, Me19), 1.47 (1 H, m, H11), 1.51 (1 H, m, H8), 1.68 (1 H, m, H15), 1.70 (1 H, m, H7α), 1.71 (1 H, m, H16), 1.72 (1 H, m, H11), 1.98 (1 H, m, H12), 2.02 (1 H, m, H23α), 2.03 (1 H, m, H20), 2.05 (3 H, s, Me28), 2.19 (1 H, m, H7β), 2.51 (1 H, m, H23β), 3.24 (1 H, br s, H6), 4.36, 4.42 (2 H, d_{AB}, $J = 13.3$ Hz, H27), 4.44 (1 H, dt, $J = 3.3$, 13.2 Hz, H22), 4.62 (1 H, d, $J = 6.0$ Hz, H4), 6.26 (1 H, d, $J = 9.8$ Hz, H2), 7.11 (1 H, dd, $J = 6.0$, 9.8 Hz, H3), OCb-4 [2.88 (3 H, s), 2.91 (3 H, s)]; ^{13}C NMR (100 MHz, $CDCl_3$) δ 11.6 (CH_3-18), 13.3 (CH_3-21), 15.5 (CH_3-19), 20.0 (CH_3-28), 21.3 (CH_2-11), 24.2 (CH_2-15), 27.3 (CH_2-16), 26.9 (CH-8), 29.8 (CH_2-23), 31.1 (CH_2-7), 38.8 (CH-20), 39.2 (CH_2-12), 42.6 (C-

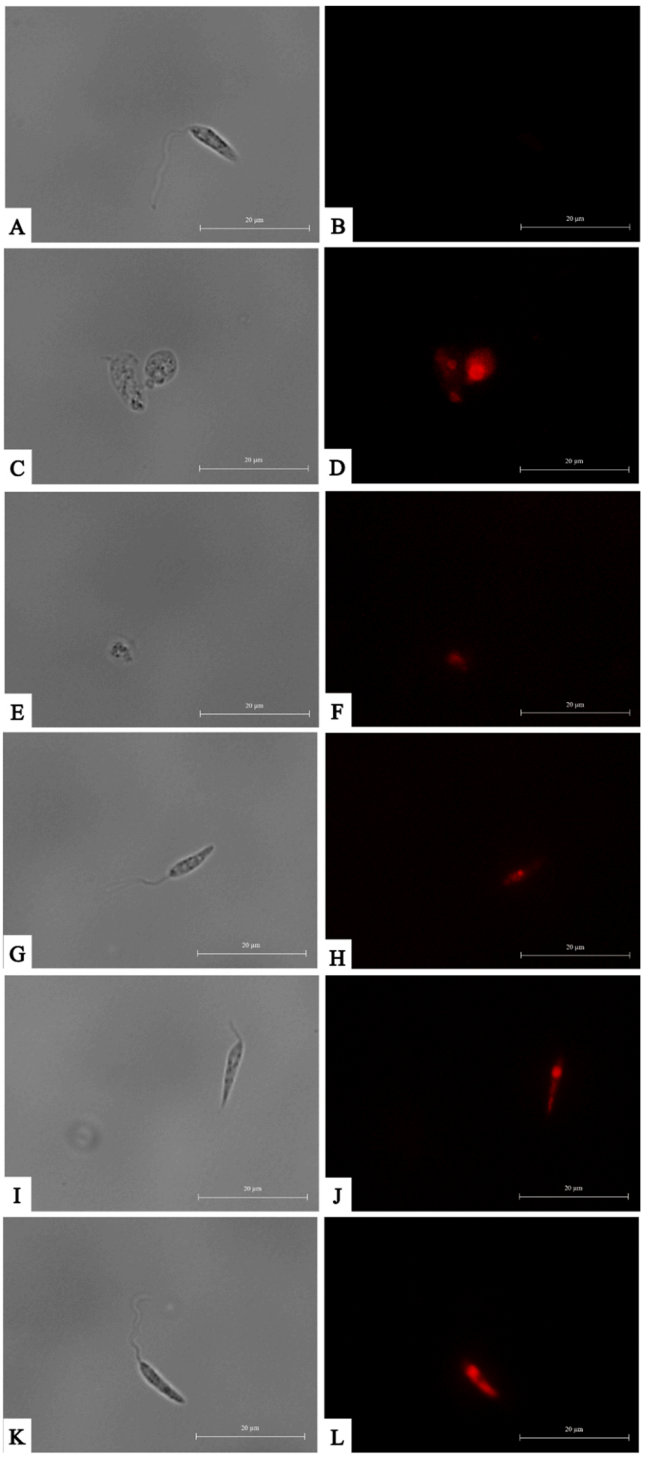

Fig. 12. Analysis of Reactive Oxygen Species in *L. amazonensis* promastigotes. Negative control of *L. amazonensis* promastigotes without treatment (A, B), positive control of *L. amazonensis* promastigotes incubated with H_2O_2 at 600 μM during 30 min (C, D), promastigotes incubated with IC_{90} of withanolide **10** (E, F), withanolide **5** (G, H), withanolide **6** (I, J) and withanolide **7** (K, L) during 24 h. The 100X images were captured using an EVOS® FL Cell Imaging System. Scale-bar: 20 μm. The assays were performed as independent experiments in triplicates.

13), 44.1 (CH-9), 48.0 (C-10), 51.9 (CH-17), 56.1 (CH-14), 57.5 (CH_2-27), 60.2 (CH-6), 61.2 (C-5), 72.7 (CH-4), 78.7 (CH-22), 125.7 (C-25), 133.4 (CH-2), 141.2 (CH-3), 152.7 (C-24), 167.0 (C-26), 201.4 (C-1), OCb-4 [36.2 (q), 36.6 (q), 155.6 (s)]; ESIMS *m/z* (%) 564 $[M+Na]^+$ (100); HRESIMS calcd for $C_{31}H_{43}NO_7Na$ $[M + Na]^+$ 564.2937, obs 564.2930.

4.1.5. Preparation of derivatives 3, 6 and 12

To a solution of **1** (40 mg, 0.09 mmol), butyric anhydride (20 μl, 0.12 mmol) was added and stirred at 0 ºC for 2 h. The residue was purified yielding compounds **3** (17.5 mg, 36 %), **6** (17.5 mg, 36 %) and **9** (5.6 mg, 10 %).

*4-O-Butyrylwithaferin A (**3**).* $[\alpha]_D^{25} = +143.4$ (*c* 2.5, $CHCl_3$); ^1H NMR (600 MHz, $CDCl_3$) δ 0.69 (3 H, s, Me18), 0.89 (1 H, m, H9), 0.94 (1 H, m, H14), 0.98 (3 H, d, $J = 6.5$ Hz, Me21), 1.08 (1 H, m, H12), 1.09 (1 H, m, H17), 1.16 (2 H, m, H15), 1.29 (1 H, m, H7α), 1.40 (1 H, m, H16), 1.38 (3 H, s, Me19), 1.43 (1 H, m, H11), 1.47 (1 H, m, H8), 1.65 (2 H, m, H15), 1.68 (1 H, m, H16), 1.71 (1 H, m, H11), 1.96 (1 H, m, H12), 2.02 (1 H, m, H20), 2.00 (1 H, m, H23α), 2.02 (3 H, s, Me28), 2.17 (1 H, m, H7β), 2.48 (1 H, m, H23β), 2.87 (1 H, t, $J = 7.0$ Hz, OH-27), 3.21 (1 H, brs, H6), 4.33 (1 H, dd, $J = 12.2$, 7.0 Hz, H27), 4.38 (1 H, dd, $J = 12.2$, 7.0 Hz, H27), 4.41 (1 H, dt, $J = 3.2$, 13.6 Hz, H22), 4.67 (1 H, d, $J = 6.1$ Hz, H4), 6.23 (1 H, d, $J = 9.8$ Hz, H2), 7.03 (1 H, dd, $J = 6.1$, 9.8 Hz, H3), OBut [0.91 (3 H, t, $J = 7.3$ Hz), 1.61 (2 H, sext, $J = 7.3$ Hz), 2.28 (2 H, t, $J = 7.3$ Hz)]; ^{13}C NMR (150 MHz, $CDCl_3$) δ 11.7 (CH_3-18), 13.5 (CH_3-21), 15.8 (CH_3-19), 20.1 (CH_3-28), 21.5 (CH_2-11), 24.4 (CH_2-15), 27.4 (CH_2-16), 29.7 (CH-8), 30.0 (CH_2-23), 31.3 (CH_2-7), 38.9 (CH-20), 39.3 (CH_2-12), 42.7 (C-13), 44.3 (CH-9), 48.2 (C-10), 52.1 (CH-17), 56.2 (CH-14), 57.6 (CH_2-27), 60.4 (CH-6), 61.2 (C-5), 72.0 (CH-4), 78.8 (CH-22), 125.9 (C-25), 133.9 (CH-2), 140.1 (CH-3), 152.9 (C-24), 167.1 (C-26), 201.3 (C-1), OBut [13.6 (q), 18.5 (t), 36.1 (t), 167.1 (s)]; ESIMS *m/z* (%) 541 $[M + H]^+$ (100); HRESIMS calcd for $C_{32}H_{45}O_7$ $[M + H]^+$ 541.3165, obs 541.3164.

4.1.6. Preparation of derivatives 9

To a solution of **1** (20 mg, 0.05 mmol), 4-nitrobenzoyl chloride (9.5 mg, 0.12 mmol) was added and stirred at room temperature for 2 h. The residue was purified yielding compounds **9** (6.1 mg, 20 %).

*27-O-(4-Nitrobenzoyl)-withaferin A (**9**).* $[\alpha]_D^{25} = +69.4$ (*c* 0.63, $CHCl_3$); ^1H NMR (500 MHz, $CDCl_3$) δ 0.71 (3 H, s, Me18), 0.97 (1 H, m, H14), 1.02 (3 H, d, $J = 6.6$ Hz, Me21), 1.04 (1 H, m, H9), 1.12 (1 H, m, H17), 1.15 (1 H, m, H12), 1.19 (1 H, m, H15), 1.29 (1 H, m, H7α), 1.41 (1 H, m, H16), 1.41 (3 H, s, Me19), 1.48 (1 H, m, H11), 1.55 (1 H, m, H8), 1.65 (2 H, m, H15), 1.71 (1 H, m, H16), 1.87 (1 H, m, H11), 1.98 (1 H, m, H12), 2.05 (1 H, m, H20), 2.10 (1 H, m, H23α), 2.15 (3 H, s, Me28), 2.17 (1 H, m, H7β), 2.59 (1 H, m, H23β), 3.23 (1 H, br s, H6), 3.76 (1 H, d, $J = 5.8$ Hz, H4), 4.43 (1 H, dt, $J = 13.4$, 3.3 Hz, H22), 5.17, 5.20 (2 H, d_{AB}, $J = 12.0$ Hz, H27), 6.20 (1 H, d, $J = 10.0$ Hz, H2), 6.93 (1 H, dd, $J = 5.8$, 10.0 Hz, H3), *p*-NO_2Bz [8.19 (2 H, d, $J = 9.0$ Hz), 8.26 (2 H, d, $J = 9.0$ Hz)]; ^{13}C NMR (125 MHz, $CDCl_3$) δ 11.8 (CH_3-18), 13.5 (CH_3-21), 17.6 (CH_3-19), 20.9 (CH_3-28), 22.4 (CH_2-11), 24.4 (CH_2-15), 27.5 (CH_2-16), 29.9 (CH-8), 30.4 (CH_2-23), 31.3 (CH_2-7), 39.0 (CH-20), 39.5 (CH_2-12), 42.8 (C-13), 44.3 (CH-9), 47.8 (C-10), 52.1 (CH-17), 56.2 (CH-14), 59.5 (CH_2-27), 62.8 (CH-6), 64.0 (C-5), 70.0 (CH-4), 77.4 (CH-22), 121.7 (C-25), 132.4 (CH-2), 142.0 (CH-3), 157.8 (C-24), 165.3 (C-26), 202.5 (C-1), *p*-NO_2Bz [123.6 (2 x CH=), 131.0 (2 x CH=), 135.5 (C=), 150.7 (C=), 164.7 (-COO-)]; ESIMS *m/z* (%) 620 $[M + H]^+$ (100); HRESIMS calcd for $C_{35}H_{42}NO_9$ $[M + H]^+$ 620.2860, obs 620.2863.

4.1.7. Preparation of derivatives 11

To a solution of **1** (20 mg, 0.05 mmol), *bromoacetyl* bromide (20 μl, 0.25 mmol) was added and stirred at room temperature for 4.5 h. The residue was purified yielding compounds **11** (8.9 mg, 31 %).

*4,27-Di-O-(bromoacetyl)-withaferin A (**11**).* $[\alpha]_D^{25} = +110.5$ (*c* 0.60, $CHCl_3$); ^1H NMR (400 MHz, $CDCl_3$) δ 0.73 (3 H, s, Me18), 0.90 (1 H, m, H9), 0.94 (1 H, m, H14), 1.02 (3 H, d, $J = 6.5$ Hz, Me21), 1.09 (1 H, m, H12), 1.10 (1 H, m, H17), 1.18 (1 H, m, H15), 1.32 (1 H, m, H7α), 1.40 (1 H, m, H16), 1.43 (3 H, s, Me19), 1.51 (1 H, m, H8), 1.52 (1 H, m, H11), 1.68 (2 H, m, H15), 1.70 (1 H, m, H11), 1.71 (1 H, m, H16), 1.97 (1 H, m, H12), 2.03 (1 H, m, H20), 2.06 (1 H, m, H23α), 2.12 (3 H, s,

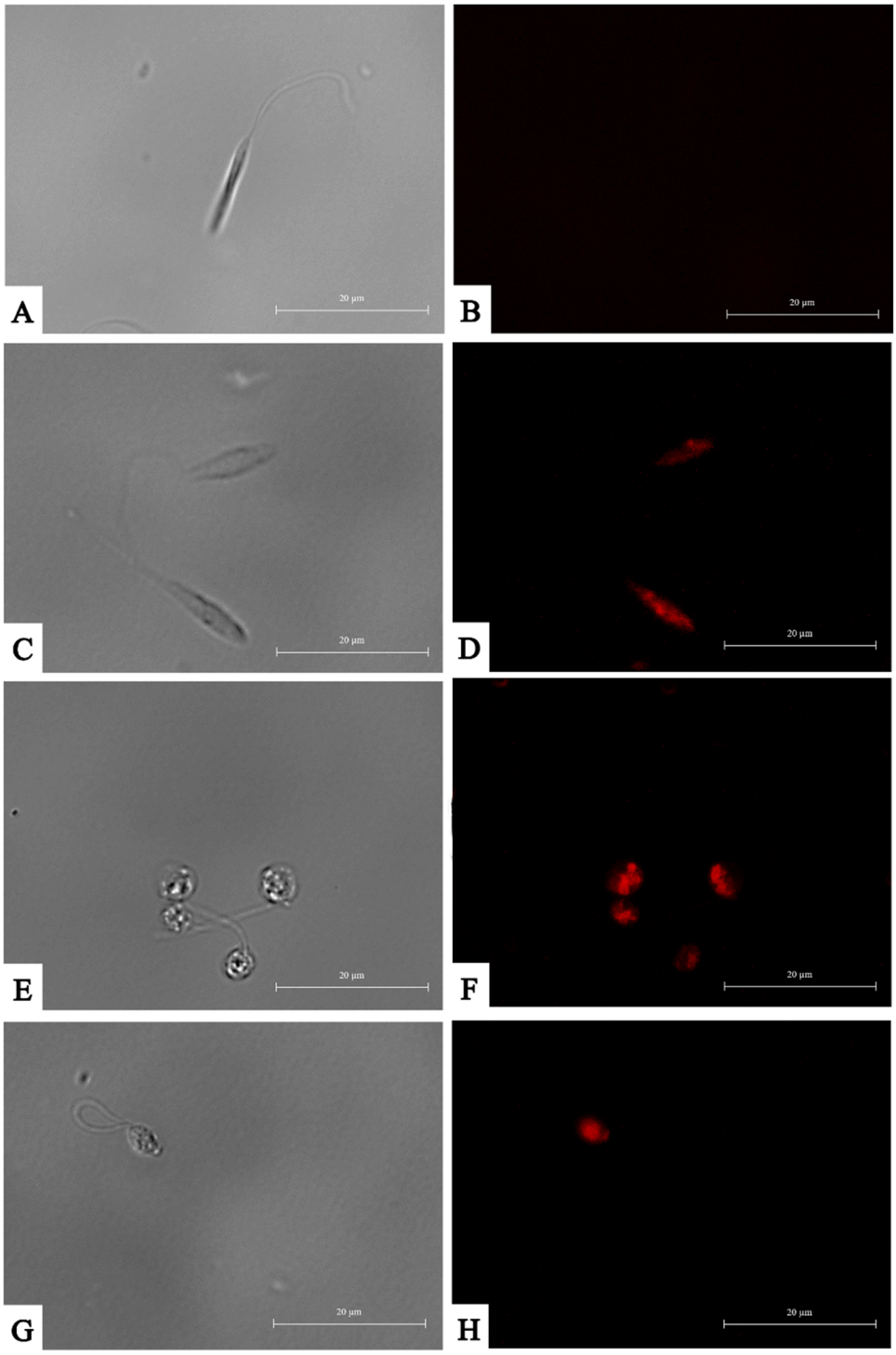

Fig. 13. Analysis of Reactive Oxygen Species in *L. donovani* promastigotes. Negative control of *L. donovani* promastigotes incubated without treatment (A, B), positive control of *L. donovani* promastigotes incubated with H_2O_2 at 600 µM during 30 min (C, D), promastigotes incubated with IC_{90} of withanolide **10** (E, F) and withanolide **3** (G, H) during 24 h. The 100X images were captured using an EVOS® FL Cell Imaging System. Scale-bar: 20 µm. These assays were performed as independent experiments in triplicates.

Me28), 2.20 (1 H, m, H7β), 2.54 (1 H, m, H23β), 3.26 (1 H, br s, H6), 4.42 (1 H, d, $J = 13.2$ Hz, H22), 4.77 (1 H, d, $J = 6.7$ Hz, H4), 4.99, 5.04 (2 H, d_{AB}, $J = 12.1$ Hz, H27), 6.32 (1 H, d, $J = 9.9$ Hz, H2), 7.04 (1 H, dd, $J = 6.7$, 9.9 Hz, H3), OBrAc [3.86 (4 H, s)]; ^{13}C NMR (100 MHz, $CDCl_3$) δ 11.6 (CH_3-18), 13.3 (CH_3-21), 15.8 (CH_3-19), 20.7 (CH_3-28), 21.4 (CH_2-11), 24.2 (CH_2-15), 27.3 (CH_2-16), 29.5 (CH-8), 30.2 (CH_2-23), 31.0 (CH_2-7), 38.7 (CH-20), 39.2 (CH_2-12), 42.6 (C-13), 44.1 (CH-9), 48.0 (C-10), 51.9 (CH-17), 56.0 (CH-14), 59.7 (CH_2-27), 60.5 (CH-6), 60.8 (C-5), 73.8 (CH-4), 78.2 (CH-22), 121.3 (C-25), 134.6 (CH-2), 138.4 (CH-3), 157.8 (C-24), 165.0 (C-26), 200.8 (C-1), OBrOAc-4 [25.2 (CH_2), 166.4 (-COO-)], OBrOAc-27 [25.8 (CH_2), 167.5 (-COO-)]; ESIMS *m/z* (%) 733 $[M + Na]^+$ (100); HRESIMS calcd for $C_{32}H_{40}O_8Br_2Na$ $[M + Na]^+$ 733.0988, obs 733.0988.

4.2. Biological cultures

To carry out the anti-leishmanial and anti-trypanosomal activity assays, promastigotes of *L. amazonensis* (MHOM/BR/77/LTB0016) and *L. donovani* (MHOM/IN/90/GE1F8R) were grown in Schneider's medium (Sigma-Aldrich, Madrid, Spain) supplemented with 10 % fetal bovine serum (VWR, Biowest, Nuaillé, France) and in RPMI 1640 medium (Gibco, Thermo Fisher, Madrid, Spain) incubated at 26 ºC.

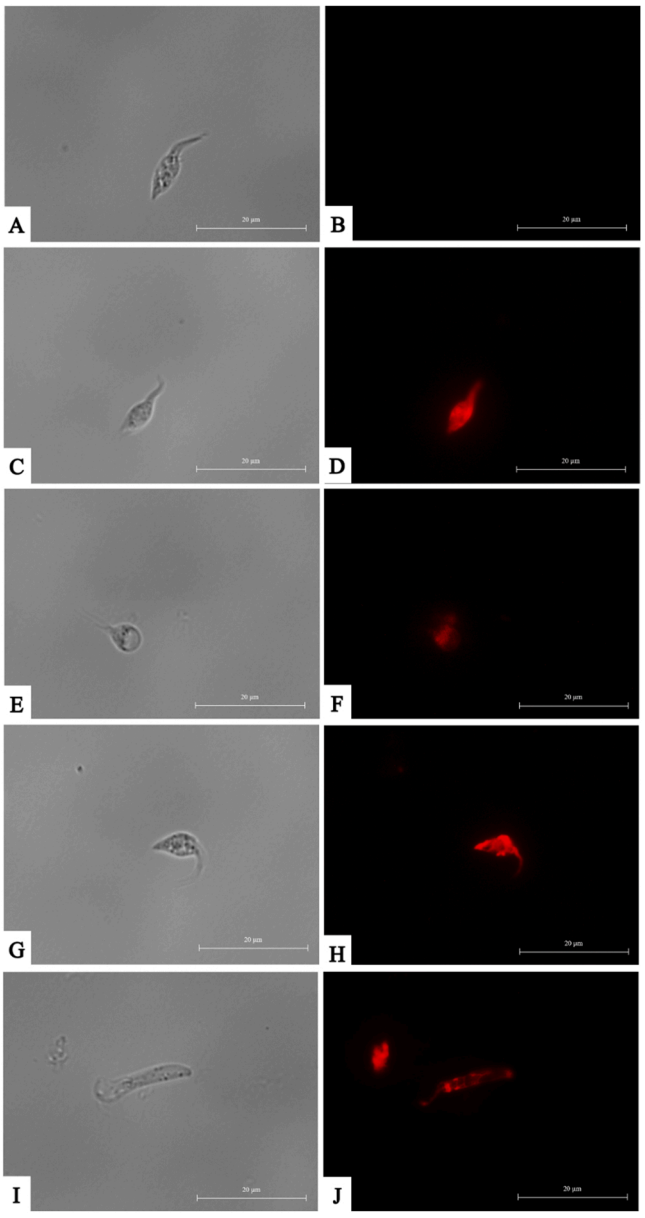

Fig. 14. Analysis of Reactive Oxygen Species in *T. cruzi* epimastigotes. Negative control of *T. cruzi* epimastigotes without treatment (A, B), positive control of *T. cruzi* epimastigotes incubated with H_2O_2 at 600 μM during 30 min (C, D), epimastigotes incubated with IC_{90} of withanolide **9** (E, F), withanolide **10** (G, H) and withanolide **6** (I, J) during 24 h. The 100X images were captured using an EVOS® FL Cell Imaging System. Scale-bar: 20 μm. These assays were performed as independent experiments in triplicates.

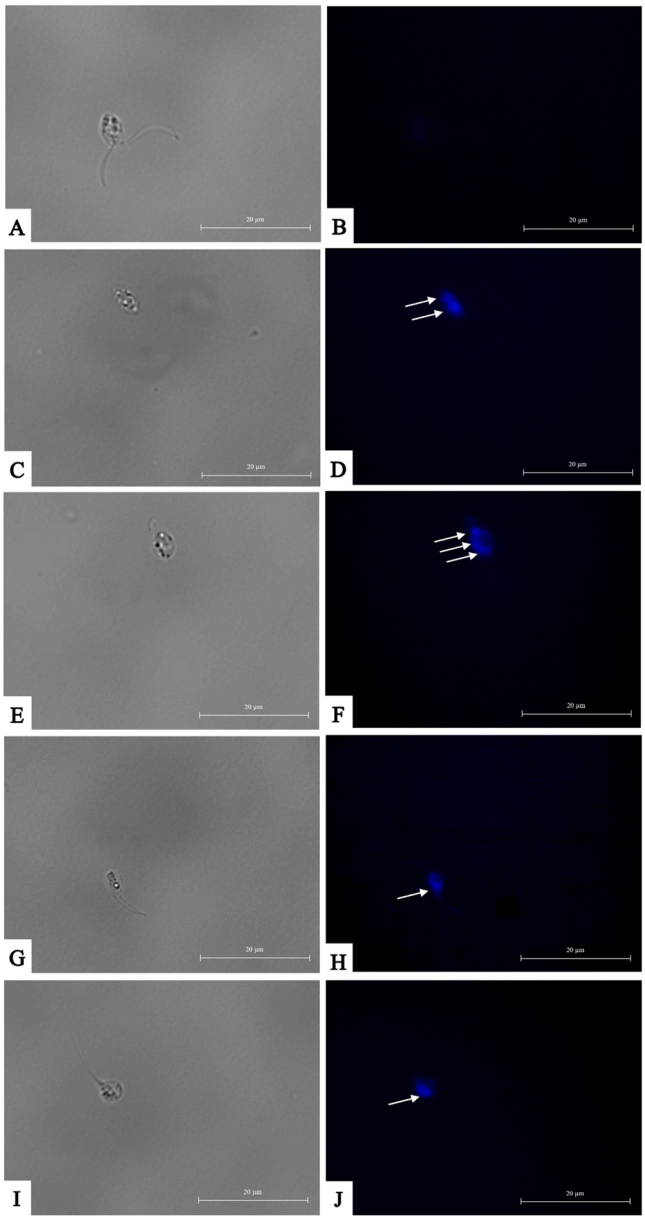

Fig. 15. Analysis of the presence of autophagic vacuoles in *L. amazonensis* promastigotes. Negative control of *L. amazonensis* promastigotes without any treatment (A, B), promastigotes incubated with IC_{90} of withanolide **10** (C, D), withanolide **5** (E, F), withanolide **6** (G, H) and withanolide **7** (I, J) during 24 h. White arrows indicate the presence of autophagic vacuoles. The 100X images were captured using an EVOS® FL Cell Imaging System. Scale-bar: 20 μm. The assays were performed as independent experiments in triplicates.

Epimastigotes of *T. cruzi* (Y strain) were incubated at the same temperature using Liver Infusion Tryptose (LIT) medium supplemented with 10 % fetal bovine serum. Dulbecco's Modified Eagle Medium (Gibco, Thermo Fisher, Madrid, Spain) supplemented with 10 % fetal bovine serumwas used to maintain the murine macrophage cell line J774A.1 (ATCC TIB-67). These cells were incubated at 37 ºC in 5 % CO_2 atmosphere. Gentamicin (Sigma-Aldrich Gentamicin solution) was added to all culture mediums up to a concentration of 10 μg/mL to avoid bacterial contamination.

4.3. Anti-leishmanial and anti-trypanosomal activity assay

Serial dilutions of the withasteroids were prepared in sterile 96-well plates. As initial activity screening concentrations, a withasteroids concentration of 100 μg/mL was used. Subsequently, as the antiparasitic activity was tested, it was necessary to decrease the initial starting concentrations of the most active analogues (starting at concentrations of 25, 12.5 and 1 μg/mL). RPMI without phenol red was used for *Leishmania* species and LIT for *T. cruzi*. *L. amazonensis* and *L. donovani* promastigotes were then added to a final concentration of 5×10^5 and *T. cruzi* epimastigotes were added to a final concentration of 2.5×10^5. Finally, 10 % alamarBlue® was added to each well and incubated for 72 h at 26 °C. The anti-leishmanial and anti-trypanosomal activity assays were based on the alamarBlue® colorimetric assay, as previously described by Núñez [40]. In order to calculate the Inhibitory Concentration 50 (IC_{50}) of the withasteroids in each of the parasites tested, fluorescence was read using the EnSpire® Multimode Plate Reader (Perkin Elmer, Madrid, Spain) and a non-linear regression analysis with

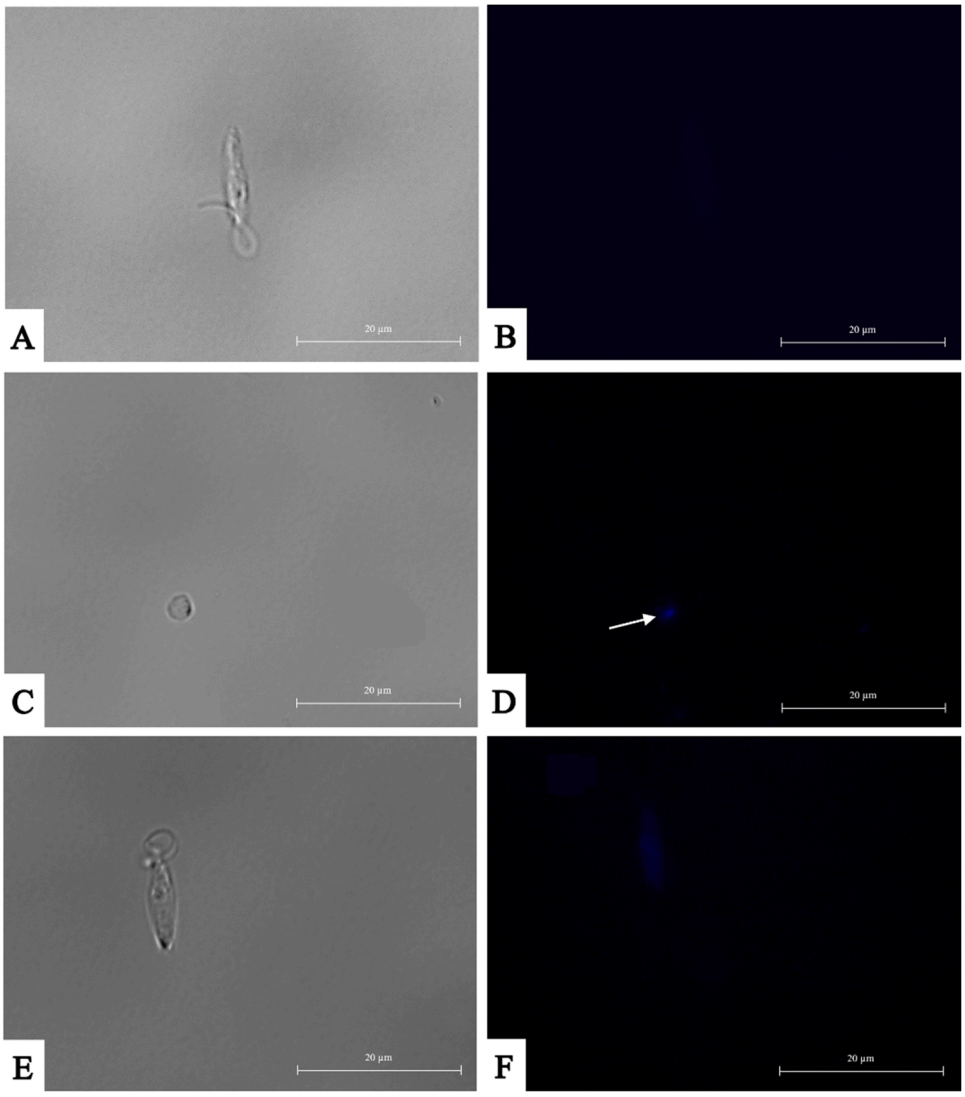

Fig. 16. Analysis of the presence of autophagic vacuoles in *L. donovani* promastigotes. Negative control of *L. donovani* promastigotes without any treatment (A, B), promastigotes incubated with IC_{90} of withanolide **10** (C, D) and withanolide **3** (E, F) during 24 h. White arrows indicate the presence of autophagic vacuoles. The 100X images were captured using an EVOS® FL Cell Imaging System. Scale-bar: 20 µm. These assays were performed as independent experiments in triplicates.

95 % confidence limits was used [41].

4.4. Anti-leishmanial activity against amastigotes stage of Leishmania amazonensis

To calculate the IC_{50} against *L. amazonensis* amastigotes, the alamarBlue® colourimetric assay was also used as previously described by Bethencourt-Estrella et al. [42]. A concentration of 10^5 murine macrophages per well was infected with a 7-day promastigote culture. The infection ratio was 1:10 (macrophages: promastigotes). Subsequently, the infected macrophages were incubated at 37 °C with 5 % CO_2 for 24 h. After this incubation time the macrophages were washed with RPMI 1640 medium and treated with withasteroids for 24 h. IC_{90} of *L. amazonensis* promastigotes were used as the starting concentration for serial dilutions. The cytotoxicity in murine macrophages was always taken into account. A 0.05 % SDS solution was then used for 30 s to rupture the macrophages and were incubated at 26 °C for 96 h. Finally, after the addition of the 10 % of alamarBlue®, fluorescence was read using the EnSpire® multimode plate reader (Perkin Elmer, Madrid, Spain). A non-linear regression analysis with 95 % confidence limits was used to calculate the IC_{50} values.

4.5. Anti-trypanosomal activity against amastigotes stage of Trypanosoma cruzi

With the target of determining the IC_{50} against *T. cruzi* amastigotes, the alamarBlue® colourimetric assay was also used as previously described. A concentration of 10^5 murine macrophages per well was infected with a 3-day epimastigote culture. In this case, the infection ratio was 1:5 (macrophages: epimastigotes). Afterward the infected macrophages were incubated at 37 °C with 5 % CO_2 for 72 h. After the incubation the macrophages were washed with DMEM and treated with withasteroids for 24 h. IC_{90} of *T. cruzi* epimastigotes were used as the starting concentration for serial dilutions. The cytotoxicity in murine macrophages was always taken into account. For the rupture of the macrophages and liberation of amastigotes, a 0.05 % SDS solution was used for 40 s and then incubated at 26 °C for 72 h using LIT. Finally, after the addition of the 10 % of alamarBlue®, fluorescence was read using the EnSpire® multimode plate reader (Perkin Elmer, Madrid, Spain) [43]. A non-linear regression analysis with 95 % confidence limits was used to calculate the IC_{50} values.

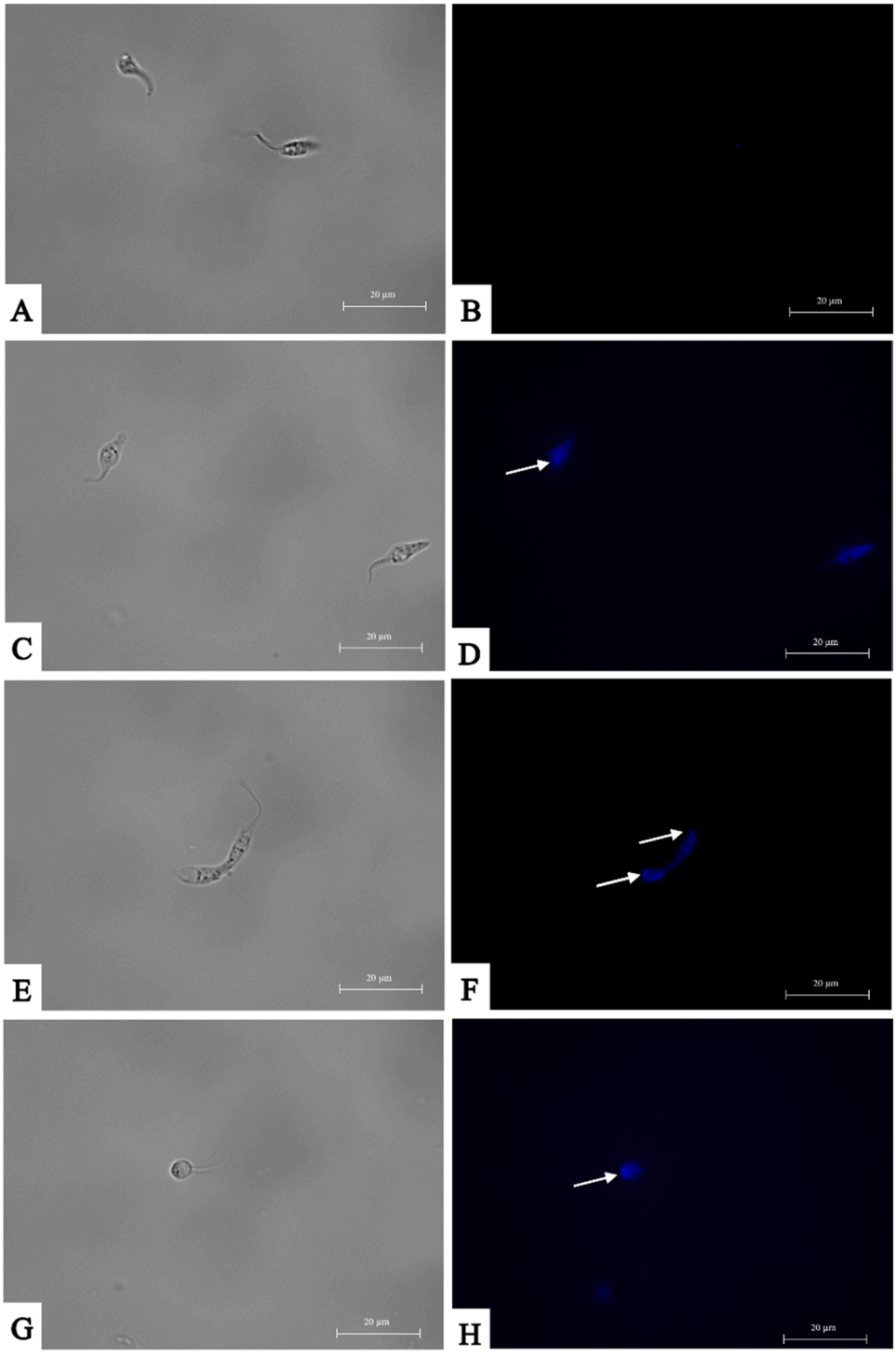

Fig. 17. Analysis of the presence of autophagic vacuoles in *T. cruzi* epimastigotes. Negative control of *T. cruzi* epimastigotes without any treatment (A, B), epimastigotes incubated with IC_{90} of withanolide **9** (C, D), withanolide **10** (E, F) and withanolide **6** (G, H) during 24 h. White arrows indicate the presence of autophagic vacuoles. The 100X images were captured using an EVOS® FL Cell Imaging System. Scalebar: 20 µm. The assays were performed as independent experiments in triplicates.

4.6. Cytotoxicity assay

10^5 murine macrophages per well were incubated with serial dilutions of the withasteroids in RPMI 1640 without phenol red. As initial activity screening concentrations, a withasteroids concentration of 400 µg/mL was used. Then 10 % alamarBlue® was added and incubated at 37 °C in a 5 % CO_2 atmosphere for 24 h. Fluorescence was measured using the EnSpire® Multimode Plate Reader (Perkin Elmer, Madrid, Spain). Finally, non-linear regression with 95 % confidence limits was used to calculate the CC_{50}.

4.7. Study of the mechanism of cell death in the parasites

To determine whether withasteroids induced programmed cell death in parasites, different experiments were carried out. To perform these experiments, *Leishmania* spp. promastigotes or *T. cruzi* epimastigotes were incubated with IC_{90} of the tested compounds at 26 °C for 24 h. Before starting each assay, parasites were centrifuged at 1500 rpm for 10 min and the pellet was resuspended in RPMI 1640 without phenol red.

4.7.1. Analysis of ATP levels

The CellTiter-Glo® luminescent cell viability assay (Promega, WI, USA) was used according to the manufacturer's instructions to determine changes in ATP levels in the parasites. The reagent in the kit is able to produce cell lysis within the treated parasites and emits a luminescence signal proportional to ATP levels. Sodium azide (NaN_3) (SIGMA) at a concentration of 20 mM was incubated with the parasites for 4.5 h as a positive control. In addition, a negative control consisting of untreated parasites was added to each experiment. After incubation of the parasites with the IC_{90} active principles and subsequent centrifugation, the pellet was resuspended in 25 μl of culture medium and transferred to a white 96-well plate. 25 μl of CellTiter-Glo kit reagent was then added, the plate was manually shaken for 2 min and allowed to stand for 10 min at room temperature in the dark. Subsequently, as described by López-Arencibia et al. luminescence was read using an EnSpire® Multimode Plate Reader (PerkinElmer, Madrid, Spain) [44]. This experiment was repeated three times and the luminescence data obtained were plotted and analysed using GraphPad.PRISM® 9.0 software. These results were expressed as percentages of ATP levels relative to the negative control. Finally, an analysis of variance by one-way ANOVA was performed using the software mentioned above.

4.7.2. Analysis of mitochondrial membrane potential

Following the manufacturer's instructions, the JC-1 Membrane Potential Assay Kit® (Cayman Chemical, Ann Arbor, MI, USA) was used to study alterations of the mitochondrial membrane potential as previously described Cartuche et al. [45]. When the mitochondrial membrane potential is under normal conditions the reagent in the kit is in dimer form that emit red fluorescence, however, when this potential is altered the reagent forms monomers that emit green fluorescence. Carbonyl cyanide 3-chlorophenylhydrazone (CCCP) 100 μM, (98 %, Thermo Scientific™) was incubated with the parasites for 3 h as a positive control. In addition, a negative control consisting of untreated parasites was added to each experiment. After incubation of the parasites with the IC_{90} compounds and subsequent centrifugation, the pellet was resuspended in 50 μl of JC-1 buffer and transferred to a black 96-well plate. 5 μl of JC-1 reagent was then added and incubated in the dark for 30 min at 26 °C. An EnSpire® Multimode Plate Reader (PerkinElmer, Madrid, Spain) was used to measure these fluorescence changes (ratio 595/535 nm). This experiment was repeated three times and the fluorescence ratios obtained were plotted and analysed using GraphPad.PRISM® 9.0 software. These results were expressed as percentages of the ratio of fluorescence intensity at 590/530 nm relative to the negative control. Analysis of variance by one-way ANOVA was also performed using the software mentioned above.

4.7.3. Analysis of plasma membrane permeability

To determine changes in cytoplasmic membrane permeability, the fluorescent dye SYTOX® Green nucleic acid stain (ThermoFisher Scientific, MA, USA) was used according to the manufacturer's instructions. Triton X-100 (SIGMA) was incubated with the parasites at a concentration of 0.1 % for 30 min as a positive control. In addition, a negative control consisting of untreated parasites was added to each experiment. The dye from the kit penetrates cells with altered plasma membrane permeability and binds to DNA. Once the dye bonds to the DNA, it can multiply its fluorescence up to 500-fold. After incubation of the parasites with IC_{90} of the compounds and subsequent centrifugation, the pellet was resuspended in 50 μl of culture medium. The treated parasites were then incubated with this fluorophore at a concentration of 1 μM at 26 ∘C for 15 min in the absence of light. After incubation, the EVOS® FL Cell Imaging System (ThermoFisher Scientific, MA, USA) was used to take images [46].

4.7.4. Chromatin condensation determination

In aim to determine chromatin condensation in treated parasites, the Vybrant® apoptosis assay kit n°5, Hoechst 33342/Propidium Iodide (ThermoFisher Scientific, MA, USA) was used according to the manufacturer's instructions. The Hoechst 33342 dye binds only to the condensed chromatin and emits an intense blue fluorescence. On the other hand, propidium iodide (PI) is able to penetrate dead cells, binds to their DNA and emits red fluorescence. In this way, it is possible to recognise three types of cell populations: with a soft blue fluorescence we would detect living cells, cells undergoing programmed cell death will fluoresce strong blue, and finally, dead cells will fluoresce high red. After incubation with the IC_{90} compounds and centrifugation, pellet was resuspended in 50 μl of culture medium. The treated parasites were incubated with Hoechst 33342 at a concentration of 5 μg/mL and PI at 1 μg/mL for 15 min in the dark at 26 ∘C as previously described Díaz Marrero et al. Finally, EVOS® FL Cell Imaging System (ThermoFisher Scientific, MA, USA) was then used to take pictures [47].

4.7.5. Analysis of reactive oxygen species

Another characteristic event of an apoptosis-like process is the accumulation of reactive oxygen species (ROS). After the parasites were incubated with the IC_{90} of the compounds and then centrifuged, pellet was resuspended in 50 μl of culture medium. CellROX® Deep Red reagent (ThermoFisher Scientific, MA, USA) was added at a concentration of 5 μM for 30 min incubation at 26 °C, following the manufacturer's instructions to determine the intracellular accumulation of ROS. With this reagent, ROS emit red fluorescence. Subsequently, images were taken using the EVOS® FL Cell Imaging System (ThermoFisher Scientific, MA, USA) [48].H_2O_2 was incubated with the parasites at a concentration of 600 μM for 30 min as a positive control. In addition, a negative control consisting of untreated parasites was added to each experiment.

4.7.6. Autophagy assay

Monodansilcadaverine (MCD), an autofluorescent dye that binds to autophagic membrane vacuoles and emits blue fluorescence, was used to reveal the presence of autophagic vacuoles [49]. This is possible due to a combination of ion sequestration and interactions with some specific lipids of the autophagic membrane.

After incubation of the parasites with the IC_{90} of the selected compounds and subsequent centrifugation, pellet was resuspended in 50 μl of culture medium. The MCD dye was added under dark conditions at a final concentration of 100 μM. After one hour of incubation, the parasites were centrifuged, and fresh medium (RPMI without phenol red) was added to reduce background. Finally, images were taken with the EVOS® FL Cell Imaging System (ThermoFisher Scientific, MA, USA).

4.8. Statistical analysis

All assays were conducted in triplicate on different days. The statistical analysis software Sigma Plot 12.0 (Systat Software) was used to calculate IC_{50} and CC_{50} values by non-linear regression with 95 % confidence limits. These results are expressed as the mean of the three replicates ± standard deviation. GraphPad.PRISM® 9.0 software program (GraphPad Software, San Diego, CA, USA) was used to represent the ATP and mitochondrial membrane potential results. Analysis of variance was determined by one-way ANOVA. Differences of $p < 0.05$ were considered statistically significant.

Statements and declarations

None.

Ethics approval

Not applicable.

Informed Consent Statement

Not applicable.

Funding

This work was funded by Instituto de Salud Carlos III, FIS (Ministerio Español de Salud, Madrid, Spain) FEDER, Spain [Project PI18/01380], Consorcio Centro De Investigacion Biomédica En Red M.P. (CIBERINFEC) de Enfermedades Infecciosas, Inst. de Salud Carlos III, Madrid, Spain [CB21/13/00100] and RICET Project [RD16/0027/0001] from Programa Redes Temáticas de Investigación Cooperativa. S.N.H.D. (TESIS2019010065) and B.E.C.J. (TESIS2020010057) was funded by a grant from the Agencia Canaria de Investigación, Innovación y Sociedad de la Información cofunded by FEDER.

CRediT authorship contribution statement

Methodology, S.N.H.D.; B.E.C.J.; L.A.A.; S.I.; Synthesis chemical compounds, H.A.E.; J.I.A.; B.I.L.; Software, S.N.H.D.; B.E.C.J.; L.A.A.; S. I.; Validation, P.J.E.; L.M.J.; J.I.A.; Formal analysis, P.J.E. and L.M.J.; Investigation, S.N.H.D.; B.E.C.J.; L.A.A.; S.I.; Resources, P.J.E.; L.M.J.; J. I.A.; Data curation, S.N.H.D.; B.E.C.J.; L.A.A.; S.I.; Writing – original draft, H.A.E.; S.N.H.D.; L.A.A.; Writing –review & editing, P.J.E.; L.M.J.; J.I.A.; Visualization, P.J.E.; L.M.J.; J.I.A.; Supervision, P.J.E. and L.M.J.; Project administration, P.J.E. and L.M.J.; Funding acquisition, P.J.E. and L.M.J. All authors have read and agreed to the published version of the manuscript.

Declaration of Competing Interest

The authors declare that they have no known competing financial interests or personal relationships that could have appeared to influence the work reported in this paper.

Acknowledgements

This work was supported by the RICET [project no. RD16/0027/0001 of the programme of Redes Temáticas de Investigación Cooperativa, FIS], CIBERINFEC de Enfermedades Infecciosas, Instituto de Salud Carlos III [CB21/13/00100], Ministerio de Sanidad, Gobierno de España and by the project N°: 21/0587 funded by the 'Cabildo de Tenerife, tenerife innova, MEDI and FDCAN. S.N.H.D. [TESIS2019010065] and B. E.C.J. [TESIS2020010057] by ACIISI, all cofounded by FEDER.

Supplementary data

^{1}H and ^{13}C NMR spectra of novel withaferin A analogues (compounds **2**, **3**, **9** and **11**). Supplementary data associated with this article can be found in the online version.

Appendix A. Supporting information

Supplementary data associated with this article can be found in the online version at doi:10.1016/j.biopha.2023.114879.

References

[1] WHO Neglected tropical diseases. In: World Health Organization. 2023. Available online: http://www.emro.who.int/health-topics/tropical-diseases/ (Accessed 03 Feb 2023).
[2] L.S. Sangenito, V. da Silva Santos, C.M. d'Avila-Levy, M.H. Branquinha, A.L. Souza Dos Santos, S.S.C. de Oliveira, Leishmaniasis and Chagas disease - neglected tropical diseases: treatment updates, Curr. Top. Med Chem. 19 (3) (2019) 174–177, https://doi.org/10.2174/1568026619031903281551 36.
[3] WHO Leishmaniasis. In: World Health Organization. 2023. Available online: https://www.who.int/news-room/fact-sheets/detail/leishmaniasis (Accessed 03 Feb 2023).
[4] WHO Chagas disease (American trypanosomiasis). In: World Health Organization. 2023. Available online: https://www.who.int/health-topics/chagas-disease#tab=tab_1 (Accessed 03 Feb 2023).
[5] Parasites-Leishmaniasis-Biology. In: Centers for Disease Control and Prevention. 2020. Available online: https://www.cdc.gov/parasites/leishmaniasis/biology.html (Accessed 03 Feb 2023).
[6] Leishmaniasis-Epidemiology & Risk Factors. In: Centers for Disease Control and Prevention. 2020. Available online: https://www.cdc.gov/parasites/leishmaniasis/epi.html (Accessed 03 Feb 2023)
[7] Parasites- American Trypanosomiasis (also known as Chagas disease)- Detailed FAQs. In: Centers for Disease Control and Prevention. 2022. Available online: https://www.cdc.gov/parasites/chagas/gen_info/detailed.html (Accessed 03 Feb 2022)
[8] Parasites- American Trypanosomiasis (also known as Chagas disease)- Disease. In: Centers for Disease Control and Prevention. 2019. Available online: https://www.cdc.gov/parasites/chagas/disease.html (Accessed 03 Feb 2023)
[9] D.S. Newman, G.M. Cragg, Natural products as sources of new drugs over the nearly four decades from 01/1981 to 09/2019, J. Nat. Prod. 83 (3) (2020) 770–803, https://doi.org/10.1021/acs.jnatprod.9b01285.
[10] A. Singh, A. Raza, S. Amin, C. Damodaran, A.K. Sharma, Recent advances in the chemistry and therapeutic evaluation of naturally occurring and synthetic withanolides, Molecules 27 (3) (2022) 886, https://doi.org/10.3390/molecules27030886.
[11] T. Sultana, M.K. Okla, M. Ahmed, N. Akhtar, A. Al-Hashimi, H. Abdelgawad, Haq Ihsan-Ul-, Withaferin A: From ancient remedy to potential drug candidate, Molecules 26 (24) (2021) 7696, https://doi.org/10.3390/molecules26247696.
[12] T. Behl, A. Sharma, L. Sharma, A. Sehgal, G. Zengin, R. Brata, O. Fratila, S. Bungau, Exploring the multifaceted therapeutic potential of Withaferin A and its derivatives, Biomedicines 8 (12) (2020) 571, https://doi.org/10.3390/biomedicines8120571.
[13] L. Basmaciyan, M. Casanova, Cell death in Leishmania, Parasite 26 (2019) 71, https://doi.org/10.1051/parasite/2019071.
[14] R.F.S. Menna-Barreto, Cell death pathways in pathogenic trypanosomatids: lessons of (over) kill, Cell Death Dis. 10 (2) (2019) 93, https://doi.org/10.1038/s41419-019-1370-2.
[15] G.G. Llanos, L.M. Araujo, I.A. Jiménez, L.M. Moujir, I.L. Bazzocchi, Withaferin A-related steroids from *Withania aristata* exhibit potent antiproliferative activity by inducing apoptosis in human tumor cells, Eur. J. Med Chem. 54 (2012) 499–511, https://doi.org/10.1016/j.ejmech.2012.05.032.
[16] G.G. Llanos, L.M. Araujo, I.A. Jiménez, L.M. Moujir, J. Rordríguez, C. Jiménez, I. L. Bazzocchi, Structure-based design, synthesis, and biological evaluation of withaferin A-analogues as potent apoptotic inducers, Eur. J. Med Chem. 140 (2017) 52–64, https://doi.org/10.1016/j.ejmech.2017.09.00.
[17] N.R. Perestelo, G.G. Llanos, C.P. Reyes, A. Amesty, K. Sooda, S. Afshinjavid, I. A. Jiménez, F. Javid, I.L. Bazzocchi, Expanding the chemical space of withaferin A by incorporating silicon to improve its clinical potential on human ovarian carcinoma cells, J. Med Chem. 62 (9) (2019) 4571–4585, https://doi.org/10.1021/acs.jmedchem.9b00146.
[18] A. López-Arencibia, D. San Nicolás-Hernández, C.J. Bethencourt-Estrella, I. Sifaoui, M. Reyes-Batlle, R.L. Rodríguez-Expósito, A. Rizo-Liendo, J. Lorenzo-Morales, I. L. Bazzocchi, J.E. Piñero, I.A. Jiménez, Withanolides from *Withania aristata* as antikinetoplastid agents through induction of programmed cell death, Pathogens 8 (4) (2019) 172, https://doi.org/10.3390/pathogens8040172.
[19] A.A. Bekhit, E. El-Agroudy, A. Helmy, T.M. Ibrahim, A. Shavandi, A.E.-D.A. Bekhit, *Leishmania* treatment and prevention: Natural and synthesized drugs, Eur. J. Med Chem. 160 (2018) 229–244, https://doi.org/10.1016/j.ejmech.2018.10.022.
[20] Y.M.B.G. de Carvalho, S. Shanmugam, M.S. Batista, M.R. Serafini, A.A.D.S. Araújo, L.J. Quintans Júnior, Pharmaceutical agents for treatment of leishmaniasis: a patent landscape, Expert Opin. Ther. Pat. 30 (8) (2020) 633–641, https://doi.org/10.1080/13543776.2020.1789100.
[21] A.G. González, J.L. Bretón, J.M. Trujillo, *Withania* steroids. III. Steroidal lactones of *Withania frutescens*, Ann. Quím. 70 (1974) 69–73.
[22] M. Suffness, J.M. Pezzuto, Assays related to cancer drug discovery, in: K. Hostettmann (Ed.), *In* Methods in plant biochemistry: Assays for bioactivity, Academic Press, London, 1991, pp. 71–133.
[23] D. San Nicolás-Hernández, C.J. Bethencourt-Estrella, A. López-Arencibia, E. Hernández-Álvarez, I. Sifaoui, I.L. Bazzocchi, J. Lorenzo-Morales, I.A. Jiménez, J.E. Piñero, Withaferin A-silyl ether analogs as potential anti-kinetoplastid agents targeting the programmed cell death, Biomed. Pharm. 157 (2023), 114012, https://doi.org/10.1016/j.biopha.2022.114012.
[24] S.C.M. Lima, J.D.S. Pacheco, A.M. Marques, E.R.P. Veltri, R.C. Almeida-Lafetá, M. R. Figueiredo, M.A.C. Kaplan, E.C. Torres-Santos, Leishmanicidal activity of Withanolides from *Aureliana Fasciculata* var. *Fasciculata*, Molecules 23 (12) (2018) 3160, https://doi.org/10.3390/molecules23123160.
[25] M. Kuroyanagi, M. Murata, T. Nakane, O. Shirota, S. Sekita, H. Fuchino, Z. K. Shinwari, Leishmanicidal active withanolides from a pakistani medicinal plant, *Withania coagulans*, Chem. Pharm. Bull. 60 (7) (2012) 892–897, https://doi.org/10.1248/cpb.c12-00264.
[26] R.B. Peres, L.F.A. Fiuza, P.B. da Silva, M.M. Batista, F.D.C. Camillo, A.M. Marques, C. de, L. Brito, M.R. Figueiredo, M.N.C. Soeiro, In vitro phenotypic activity and in silico analysis of natural products from brazilian biodiversity on *Trypanosoma cruzi*, Molecules 26 (18) (2021) 5676, https://doi.org/10.3390/molecules26185676.
[27] S. Nagafuji, H. Okabe, H. Akahane, F. Abe, Trypanocidal constituents in plants 4. Withanolides from the aerial parts of *Physalis angulata*, Biol. Pharm. Bull. 27 (2) (2004) 193–197, https://doi.org/10.1248/bpb.27.193.

[28] S. Kaczanowski, M. Sajid, S.E. Reece, Evolution of apoptosis-like programmed cell death in unicellular protozoan parasites, Parasit. Vectors 4 (2011) 44, https://doi.org/10.1186/1756-3305-4-44.
[29] L.M. Fidalgo, L. Gille, Mitochondria and trypanosomatids: targets and drugs, Pharm. Res 28 (11) (2011) 2758–2770, https://doi.org/10.1007/s11095-011-0586-3.
[30] V. Guhe, F. Anjum, A. Shafie, M.I. Hassan, V.R. Pasupuleti, S. Singh, Infection dynamics of ATG8 in *Leishmania*: balancing autophagy for therapeutics, Molecules 27 (10) (2022) 3142, https://doi.org/10.3390/molecules27103142.
[31] D. Arnoult, K. Akarid, A. Grodet, P.X. Petit, J. Estaquier, J.C. Ameisen, On the evolution of programmed cell death: apoptosis of the unicellular eukaryote *Leishmania major* involves cysteine proteinase activation and mitochondrion permeabilization, Cell Death Differ. 9 (1) (2002) 65–81, https://doi.org/10.1038/sj.cdd.4400951.
[32] C.M. Adade, G.S. Chagas, T. Souto-Padrón, *Apis mellifera* venom induces different cell death pathways in *Trypanosoma cruzi*, Parasitology 139 (11) (2012) 1444–1461, https://doi.org/10.1017/S0031182012000790.
[33] J. Dhami, E. Chang, S.S. Gambhir, Withaferin A and its potential role in glioblastoma (GBM, J. Neurooncol. 131 (2) (2017) 201–211, https://doi.org/10.1007/s11060-016-2303-x.
[34] S. Bungau, C.M. Vesa, A. Abid, T. Behl, D.M. Tit, A.L. Purza, B. Pasca, L.M. Todan, L. Endres, Withaferin A-a promising phytochemical compound with multiple results in dermatological diseases, Molecules 26 (9) (2021) 2407, https://doi.org/10.3390/molecules26092407.
[35] N. Sen, B. Banerjee, B.B. Das, A. Ganguly, T. Sen, S. Pramanik, S. Mukhopadhyay, H.K. Majumder, Apoptosis is induced in leishmanial cells by a novel protein kinase inhibitor withaferin A and is facilitated by apoptotic topoisomerase I-DNA complex, Cell Death Differ. 14 (2) (2007) 358–367, https://doi.org/10.1038/sj.cdd.4402002.
[36] A. Grover, S.P. Katiyar, J. Jeyakanthan, V.K. Dubey, D. Sundar, Blocking protein kinase C signaling pathway: mechanistic insights into the anti-leishmanial activity of prospective herbal drugs from *Withania somnifera*, BMC Genom. 13 (2012) S20, https://doi.org/10.1186/1471-2164-13-S7-S20.
[37] S. Chandrasekaran, A. Dayakar, J. Veronica, S. Sundar, R. Maurya, An *in vitro* study of apoptotic like death in *Leishmania donovani* promastigotes by withanolides, Parasitol. Int. 62 (3) (2013) 253–261, https://doi.org/10.1016/j.parint.2013.01.007.
[38] Y.Y. Jung, J.Y. Um, A. Chinnathambi, C. Govindasamy, A.S. Narula, O. A. Namjoshi, B.E. Blough, G. Sethi, K.S. Ahn, Withanolide modulates the potential crosstalk between apoptosis and autophagy in different colorectal cancer cell lines, Eur. J. Pharm. 928 (2022), 175113, https://doi.org/10.1016/j.ejphar.2022.175113.
[39] P. Das, S. Saha, S. BoseDasgupta, The ultimate fate determinants of drug induced cell-death mechanisms in Trypanosomatids, Int J. Parasitol. Drugs Drug Resist. 15 (2021) 81–91, https://doi.org/10.1016/j.ijpddr.2021.01.003.
[40] M.J. Núñez, M.L. Martínez, A. López-Arencibia, C.J. Bethencourt-Estrella, D. San Nicolás-Hernández, I.A. Jiménez, J. Lorenzo-Morales, J.E. Piñero, I.L. Bazzocchi, *In vitro* susceptibility of kinetoplastids to celastroloids from *Maytenus chiapensis*, Antimicrob. Agents Chemother. 65 (6) (2021), https://doi.org/10.1128/AAC.02236-20.
[41] X. Zhang, A.K. Samadi, K.F. Roby, B. Timmermann, M.S. Cohen, Inhibition of cell growth and induction of apoptosis in ovarian carcinoma cell lines CaOV3 and SKOV3 by natural withanolide Withaferin A, Gynecol. Oncol. 124 (3) (2012) 606–612, https://doi.org/10.1016/j.ygyno.2011.11.044.
[42] C.J. Bethencourt-Estrella, N. Nocchi, A. López-Arencibia, D. San Nicolás-Hernández, M.L. Souto, B. Suárez-Gómez, A.R. Díaz-Marrero, J.J. Fernández, J. Lorenzo-Morales, J.E. Piñero, Antikinetoplastid activity of sesquiterpenes isolated from the zoanthid *Palythoa aff. clavata*, Pharmaceuticals 14 (11) (2021) 1095, https://doi.org/10.3390/ph14111095.
[43] C.J. Bethencourt-Estrella, S. Delgado Hernández, A. López-Arencibia, D. San Nicolás-Hernández, D. Tejedor, F. García Tellado, J. Lorenzo-Morales, J.E. Piñero Barroso, In vitro activity and mechanism of cell death induction of cyanomethyl vinyl ethers derivatives against Trypanosoma cruzi, Int. J. Parasitol. Drugs Drug Resist. (2023).
[44] A. López-Arencibia, C. Martín-Navarro, I. Sifaoui, M. Reyes-Batlle, C. Wagner, J. Lorenzo-Morales, S.K. Maciver, J.E. Piñero, Perifosine mechanisms of action in *Leishmania* species, Antimicrob. Agents Chemother. 61 (4) (2017) e02127–16, https://doi.org/10.1128/AAC.02127-16.
[45] L. Cartuche, I. Sifaoui, A. López-Arencibia, C.J. Bethencourt-Estrella, D. San Nicolás-Hernández, J. Lorenzo-Morales, J.E. Piñero, A.R. Díaz-Marrero, J. J. Fernández, Antikinetoplastid activity of indolocarbazoles from *Streptomyces sanyensis*, Biomolecules 10 (4) (2020) 657, https://doi.org/10.3390/biom10040657.
[46] C.J. Bethencourt-Estrella, S. Delgado-Hernández, A. López-Arencibia, D. San Nicolás-Hernández, I. Sifaoui, D. Tejedor, F. García-Tellado, J. Lorenzo-Morales, J. E. Piñero, Acrylonitrile derivatives against *Trypanosoma cruzi*: *In vitro* activity and programmed cell death study, Pharmaceuticals 14 (6) (2021) 552, https://doi.org/10.3390/ph14060552.
[47] A.R. Díaz-Marrero, A. López-Arencibia, C.J. Bethencout-Estrella, F. Cen-Pacheco, I. Sifaoui, A. Hernández Creus, M.C. Duque-Ramírez, M.L. Souto, A. Hernández Daranas, J. Lorenzo-Morales, J.E. Piñero, J.J. Fernández, Antiprotozoal activities of marine polyether triterpenoids, Bioorg. Chem. 92 (2019), 103276, https://doi.org/10.1016/j.bioorg.2019.103276.
[48] I. Sifaoui, I. Rodríguez-Talavera, M. Reyes-Batlle, R.L. Rodríguez-Expósito, P. Rocha-Cabrera, J.E. Piñero, J. Lorenzo-Morales, *In vitro* evaluation of commercial foam Belcils® on *Acanthamoeba* spp, Int. J. Parasitol. Drugs Drug Resist. 14 (2020) 136–143, https://doi.org/10.1016/j.ijpddr.2020.10.002.
[49] C.M. Adade, G.S. Chagas, T. Souto-Padrón, *Apis mellifera* venom induces different cell death pathways in *Trypanosoma cruzi*, Parasitology 139 (11) (2012) 1444–1461, https://doi.org/10.1017/S0031182012000790.